UCLA
UCLA Previously Published Works

Title

Decentralized observers with consensus filters for distributed discrete-time linear systems

Permalink
https://escholarship.org/uc/item/4pz9j09z

Journal
Automatica, 50(4)

ISSN
0005-1098

Authors
Açıkmeşe, Behçet
Mandić, Milan
Speyer, Jason L

Publication Date
2014-04-01

DOI
10.1016/j.automatica.2014.02.008

Peer reviewed

eScholarship.org Powered by the California Digital Library
University of California

Automatica 50 (2014) 1037–1052

Contents lists available at ScienceDirect

Automatica

journal homepage: www.elsevier.com/locate/automatica

Decentralized observers with consensus filters for distributed discrete-time linear systems ☆

Behçet Açıkmeşe [a,1], Milan Mandić [b], Jason L. Speyer [c]

[a] Aerospace Engineering and Engineering Mechanics, The University of Texas at Austin, 210 E.24th St., Austin, TX 78712, USA
[b] Jet Propulsion Laboratory, California Institute of Technology, 4800 Oak Grove Drive, Pasadena, CA 91109, USA
[c] Mechanical & Aerospace Engineering, University of California, 420 Westwood Plaza, 38-137O, Los Angeles, CA 90095, USA

ARTICLE INFO

Article history:
Received 20 December 2011
Received in revised form
15 September 2013
Accepted 4 January 2014
Available online 24 February 2014

Keywords:
Observers
Distributed systems
Graph theory
Linear matrix inequalities

ABSTRACT

This paper presents a decentralized observer with a consensus filter for the state observation of discrete-time linear distributed systems. Each agent in the distributed system has an observer with a model of the plant that utilizes the set of locally available measurements, which may not make the full plant state detectable. This lack of detectability is overcome by utilizing a consensus filter that blends the state estimate of each agent with its neighbors' estimates. It is proven that the state estimates of the proposed observer exponentially converge to the actual plant states under arbitrarily changing, but connected, communication and pseudo-connected sensing graph topologies. Except these connectivity properties, full knowledge of the sensing and communication graphs is not needed at the design time. As a byproduct, we obtained a result on the location of eigenvalues, i.e., the spectrum, of the Laplacian for a family of graphs with self-loops.

© 2014 Elsevier Ltd. All rights reserved.

1. Introduction

Decentralized estimation (Siljak, 1978) has long been an active area of research with an increased recent interest in distributed systems. This paper focuses on a decentralized observer problem for a distributed system with multiple agents, where each agent represents a physical entity such as an aircraft in a formation. In the context of the observer synthesis problem, having a decentralized observer implies that each agent has a local observer that computes the estimate of the whole system state with locally available measurements and communicated data with its neighbors. Having a distributed system means that the local measurements available to the agents do not provide full state observability at the agent level, and measurements of all agents collectively make the full state observable.

Some of the earlier research in decentralized estimation focused on combining the state estimates of a system with multiple agents into a single central estimate (Mutambara, 1998; Speyer, 1979; Willsky, Bello, Castanon, Levy, & Verghese, 1982), where all the information is communicated to all agents back and forth. Since this approach requires fully connected communication network and with possibly high volume of communication, it may not be appropriate for distributed systems with a large number of agents. The main idea behind these algorithms is to blend independently obtained state estimates into a single better state estimate, which has been the main idea behind the more recent algorithms as well. In the covariance intersection method described in Arambel, Rago, and Mehra (2001) and Chen, Arambel, and Mehra (2002), the state estimates and their error covariance matrices are exchanged without the exact knowledge of correlation between the estimates of the different agents. The unknown correlation between the exchanged state estimates is bounded by a bound on the intersection of the error covariance matrices. This method ensures that the unknown correlations are accounted for, but it requires the computation of the error covariances and their inverses, which can be computationally demanding. In a recent approach to distributed system state estimation, Shi, Johansson, and Murray (2008) considered a fusion center that combines measurements or state estimates from the agents into a single estimate by

☆ The material in this paper was partially presented at the 2011 American Control Conference (ACC 2011), June 29–July 1, 2011, San Francisco, California, USA. This paper was recommended for publication in revised form by Associate Editor Valery Ugrinovskii under the direction of Editor Ian R. Petersen.

E-mail addresses: behcet@austin.utexas.edu (B. Açıkmeşe), Milan.Mandic@jpl.nasa.gov (M. Mandić), speyer@seas.ucla.edu (J.L. Speyer).

[1] Tel.: +1 626 3181002; fax: +1 512 471 3788.

http://dx.doi.org/10.1016/j.automatica.2014.02.008
0005-1098/© 2014 Elsevier Ltd. All rights reserved.

using a Kalman filter with a particular structure. However we have to treat each agent as a fusion center if this approach is to be adapted, which increases the complexity of the information routing problem. Clearly this alternative approach may be more desirable in some applications. Hence we do not claim that our consensus based approach is a better design option for all possible decentralized observation problems. Our objective is to establish a rigorous analysis method for consensus based observer synthesis that may aid engineers to make the best specific design choices. A large number of recent research study the consensus problems in distributed control systems in a graph theoretical framework (Das & Mesbahi, 2006; Hatano & Mesbahi, 2005; Olfati-Saber, Fax, & Murray, 2007; Olfati-Saber & Murray, 2004; Ren & Beard, 2005; Smith & Hadaegh, 2007; Xiao, Boyd, & Kim, 2007). The distributed Kalman filters with embedded consensus filters are studied by Olfati-Saber (2005) and Olfati-Saber (2007). Particularly, Olfati-Saber (2007) introduces a state estimator for continuous-time linear systems with a consensus filter that blends state estimates of neighboring agents, which motivated the particular observer structure we adapted in this paper.

In this paper we consider a Linear Matrix Inequality (LMI) approach for designing observers with consensus filters for linear decentralized systems, where we explicitly construct quadratic Lyapunov functions to prove the exponential stability of the proposed decentralized observer under time varying measurement and communication topologies. LMI based centralized observer design is considered for a general class of continuous-time systems with nonlinear and time-varying terms satisfying incremental quadratic inequalities (Açıkmeşe & Corless, 2011). LMI based decentralized estimators are considered in Subbotin and Smith (2009) for fixed and stochastic communication networks. In our observer architecture, each agent utilizes its local measurements and its neighbors' communicated state estimates to update its own state estimate, which makes the information routing problem straight-forward. The locally available measurement vectors are described linearly as a function of the plant state via time-varying matrices. The local measurements alone *do not* provide the full state detectability that is required to have exponentially convergent local observers. Thus, each agent uses a consensus filter to blend the state estimates with its neighbors' estimates in order to achieve a consensus among agents, which ultimately resolves this lack of local detectability. The consensus filters update their internal states more frequently then the local observers, i.e., there are multiple consensus updates in between the observer state updates that utilize the locally available measurements. This ensures that a sufficient level of consensus is reached for the stability of the observers. For the proof of this, the overall error dynamics is first split into an *agreement* and *disagreement* subspaces. First we prove the exponential stability of the error dynamics in the agreement subspace via a quadratic Lyapunov function, where the agreement dynamics is captured via a norm bounded linear differential inclusion (Boyd, El Ghaoui, Feron, & Balakrishnan, 1994) that properly accounts for all possible changes in the sensing topology. The Lyapunov function is constructed by using LMIs and a new graph theoretic result (a byproduct of this research) on the spectrum of the Laplacian matrices corresponding to the undirected sensing graphs with self-loops, which can be found in the Appendix. We establish a *single* LMI-synthesis condition, which guarantees the resulting observer has exponentially stable agreement error dynamics for all possible time-varying sensing topologies. This LMI-synthesis requires solution of several LMIs for the proposed observer. The number of LMIs is a constant, and is independent of the number of the possible sensing and communication topologies and the number of agents. In the second step, we establish a sufficient number of consensus updates between each consecutive pair of measurement updates to ensure the disagreement error dynamics is driven to the origin. An upper bound on the number of consensus updates needed is quantified by considering the agreement and the disagreement dynamics as two interconnected systems and by utilizing a small gain type of argument.

It is important to note that the proposed observer construction and its proof are non-trivial that requires overcoming several difficulties. The first difficulty is establishing a proof of the observer stability when all the measurements are available to a single agent, before we establish the proof for the decentralized case. For example if we use a Kalman filter for a discrete linear system, there are observability and controllability conditions for stability that are nontrivial to establish when any of the system matrices are time varying (e.g., see Theorem 7.4 in Anderson & Moore, 1979 or Jazwinski, 1970), which is the case here due to changes in the sensing topology. Furthermore obtaining a Lyapunov function proving stability is an additional difficulty. The second difficulty is establishing the exponential stability of the decentralized observer, where each agent utilizes only a subset of measurements and the estimates of its neighboring agents. Particularly obtaining a sufficient upper bound on the number of consensus updates (between consecutive measurement updates) proved to be one of the main challenges. Note that this is not a difficulty in continuous-time case, since the consensus speed can arbitrarily be increased by simply adjusting a scalar design parameter (Olfati-Saber, 2007), which is indeed the main challenge in going from continuous to discrete-time design. In Kamgarpour and Tomlin (2008) a decentralized Kalman filter with consensus is introduced. The stability is ensured only for inherently stable linear systems, which is a constraining assumption, that is relaxed in the current paper so that the decentralized estimator can be applied to many practical engineered systems. This relaxation brought many new technical challenges and increased the complexity of our analysis to obtain a more general result. A decentralized estimation architecture with multiple consensus steps between measurement updates is also considered in Khan and Jadbabaie (2011) for linear systems with time-invariant sensing and communication graphs. The time-invariance eliminated the key complications and challenges faced in the current paper that considers time-varying sensing and communication graphs, which are not known ahead of time.

In summary, the main contributions of this paper are: (i) The introduction of multiple consensus updates (repetitive consensus) between measurement updates in the discrete-time decentralized observers. (ii) A proof of the exponential stability of the observer error dynamics, with repetitive consensus, under time-varying communication and sensing topologies and without their full knowledge. (iii) An explicit quantification of the number of consensus updates between two consecutive measurement updates sufficient for the exponential stability of the error dynamics. (iv) Introduction of pseudo-connected graphs, which was instrumental in our developments and which we believe can be useful in multi-agent system theory in general. (v) A useful result on the eigenvalues of Laplacians of pseudo-connected graphs. We believe that this mathematical result is interesting and useful in graph theory, independent of its specific use in the current paper. Simulation results of a group of spacecraft are presented to demonstrate the observer design procedure and the performance of the resulting decentralized observer.

Notation: The following is a partial list of notation (see the Appendix for the graph theoretic notation): $\mathbb{R}^n$ is the n dimensional real vector space; $\|\cdot\|$ is the vector 2-norm; I is the identity matrix and I_m is the identity matrix in $\mathbb{R}^{m\times m}$; $\mathbf{1}_m$ is a vector of ones in $\mathbb{R}^m$; $\mathbf{e}_i$ is a vector with its ith entry $+1$ and the others zeros; $\sigma(A)$ is the set of eigenvalues of A; $\sigma_+(S)$ are the positive eigenvalues of $S = S^T$; $\rho(A)$ is the spectral radius of A; "$\otimes$" is the Kronecker product; $(v_1, \ldots, v_m)$ is a vector obtained by augmenting vectors $v_1, \ldots, v_m$: $(v_1, \ldots, v_m) \equiv [v_1^T \ldots v_m^T]^T$; $Q = Q^T > (\geq) 0$ implies Q is a symmetric positive (semi-)definite matrix; for $P = P^T > 0$,

P-norm of a vector q is given by $\|q\|_P = \|P^{\frac{1}{2}}q\|$ and P-norm of a square matrix Q is given by $\|Q\|_P = \|P^{\frac{1}{2}}QP^{-\frac{1}{2}}\|$.

1.1. System description

We consider the problem of decentralized state observation for the following discrete-time linear system representing a group of N collaborative agents:

$$x_{k+1} = Ax_k \tag{1}$$

$$y_{i,k} = C_{i,k}x_k, \quad i = 1, \ldots, N \tag{2}$$

where $x_k \in \mathbb{R}^n$ is the state vector at time instance k and $y_{i,k} \in \mathbb{R}^{m_{i,k}}$ is the measurement vector of the ith agent at time instance k. In upcoming discussions, the index "i" is typically the index for an agent and "k" is the index for a time instance. In this scenario, each agent has its own measurements determined by the measurement matrix $C_{i,k}$ and it has direct communication links with a subset of other agents, which will be referred as the "neighbors". The set of communication links in between the agents determine the communication topology and an associated graph, $\mathbf{G}_{c,k}$, where each agent is represented by a vertex of $\mathbf{G}_{c,k}$, and each communication link is represented by an edge of $\mathbf{G}_{c,k}$. We assume that the graph $\mathbf{G}_{c,k}$ is a *undirected connected* graph (Deo, 1974) without self-loops or multiple edges for all times, which implies that (Fiedler, 1973) $\mathbf{a}(\mathbf{G}_{c,k}) > 0$ for all $k = 0, 1, \ldots$ (see the Appendix for the definition of algebraic connectivity $\mathbf{a}$). The construction of a sensing graph is more complex. To do that, we consider a "core" set of m measurements z_k,

$$z_k = \begin{bmatrix} z_{1,k} \\ \vdots \\ z_{m,k} \end{bmatrix} = Cx_k \quad \text{where } C = \begin{bmatrix} C_1 \\ \vdots \\ C_m \end{bmatrix}, \; z_{i,k} \in \mathbb{R}^p \forall\, i \tag{3}$$

such that all locally available "actual" measurements are formed as a linear combination of the core measurements:

$$y_{i,k} = \left(E_{i,k} \otimes I_p\right) z_k \Rightarrow C_{i,k} = (E_{i,k} \otimes I_p)C, \quad \forall i, \tag{4}$$

where $E_{i,k} \in \mathbb{R}^{q_{i,k} \times m}$, $i = 1, \ldots, N$, are "vertex–edge adjacency" matrices, hence $m_{i,k} = q_{i,k}p$, i.e., the size of local measurement vectors is an integer multiple of p for all agents. The vertex–edge adjacency matrix of a graph is different from its incidence matrix. Each row of the vertex–edge adjacency matrix describes an edge between two vertices with entries corresponding to these vertices are $+1$ and -1 (it does not matter which entry is $+$ or $-$) and the rest of the entries are zeros. Note that if the edge described by a row is a self-loop then there is only one non-zero entry with $+1$. In contrary each column of the incidence matrix describes an edge with $+1$ entries corresponding to both vertices. Hence a row of $E_{i,k}$, denoted by π, defining an edge between pth and qth vertices of the graph has its jth entry of π_j as follows

$$\pi_j = \begin{cases} 1 & j = p \\ -1^{(q-p)} & j = q \\ 0 & \text{otherwise.} \end{cases}$$

The assumption that all actual measurements can be expressed in terms of the core measurements adds more structure to the problem at hand without losing generality, and its use will become apparent in later sections. For example, in spacecraft example given in Section 7, the set of core measurements is the position of each spacecraft relative to a leader spacecraft. All other relative positions are linear combinations of the relative positions to the leader, i.e., the core measurements.

Next we collect the set of all distinct local measurements into a global measurement vector y_k as follows

$$y_k = (E_k \otimes I_p)\, z_k = (E_k \otimes I_p)\, Cx_k, \tag{5}$$

where the vertex–edge adjacency matrix E_k contains all the distinct rows of all $E_{i,k}$, $i = 1, \ldots, N$, that is, E_k is a vertex–edge adjacency matrix of a graph without multiple edges. Therefore, y_k is not necessarily an augmentation of all local measurements in general, that is, $y_k \neq (y_{1,k}, \ldots, y_{N,k})$ in general. Moreover a local measurement vector $y_{i,k}$ for any agent can simply be obtained by picking the right entries of the vector y_k. Consequently, a row of E_k can correspond to a measurement that belongs to multiple agents. For each agent we will define a vector $h_{i,k} \in \mathbb{Z}^{q_{i,k}}$ that contains the positive integer numbers representing how many agents each measurement is available to. This implies that

$$\mathcal{L}(\mathbf{G}_{s,k}) = E_k^T E_k = \sum_{i=1}^{N} E_{i,k}^T \left(\mathrm{diag}(h_{i,k})\right)^{-1} E_{i,k} \tag{6}$$

where $\mathcal{L}(\mathbf{G}_{s,k})$ is the sensing graph Laplacian with possibly self-loops but with the effects of multiple-edges removed by dividing the expression with $\mathrm{diag}(h_{i,k})$. Without this division, since a measurement can be available to multiple agents, the Laplacian would have accounted for multiple edges between two vertices. In summary, the sensing graph $\mathbf{G}_{s,k}$ is constructed with its vertices as the core set of measurements $z_{1,k}, \ldots, z_{m,k}$ and its edges represent the actual measurements at time instance k. Since a core measurement can also be an actual measurement, e.g., $y_{i,k} = z_{j,k}$, a sensing graph can have self loops, and in the case when all measurements are the core ones, the sensing graph can be completely disconnected in the usual sense. We introduce a concept of *pseudo-connected* graphs to capture useful properties of the sensing graphs that will be encountered (see Fig. 13 in the Appendix for an example). Given Definition 1 in the Appendix, the following conditions are assumed to hold for the system defined by Eqs. (1) and (2):

(A1) $\mathbf{G}_{c,k}$ is a connected graph without self-loops or multiple edges $\forall k$.
(A2) $\mathbf{G}_{s,k}$ is pseudo-connected without multiple edges $\forall k$ (see the Definition 1 in the Appendix).
(A3) The pair (C, A) is detectable.
(A4) ith agent knows $h_{i,k}$ for $y_{i,k}$ for any k and i.

Assuming a pseudo-connected sensing graph implies that one or more of the core measurements are among the actual measurements at any given time. As will be apparent in Section 4, the main reason behind this assumption is to establish the exponential stability of the observation error dynamics in the agreement subspace, which is the subspace where all observer estimates are the same.

Having connected communication graphs can be relaxed to, for example, having jointly connected communication graphs (Jadbabaie, Lin, & Morse, 2003). Such relaxations can lead to some generalizations of the forthcoming results, which is not discussed further in this paper. The detectability of (C, A) pair ensures that an exponentially stable observer exists by utilizing only the core measurements.

The assumption of each agent having the information of $h_{i,k}$ means that each agent knows how many other agents have access to the same information. The $h_{i,k}$ values can simply be available to each agent that has a measurement, or the distributed system may have the working assumption that each measurement is known by a fixed number of agents.

2. Decentralized observer with a consensus filter

This section introduces the following local observers with a consensus filter, which is our first contribution, that process both the locally available measurements and the neighbors' state estimates:

Decentralized Observers with Consensus Filter

$$\hat{x}_{i,k+1} = As_{i,k} + L_{i,k}(C_{i,k}s_{i,k} - y_{i,k}) \quad (7)$$

$$\xi_{i,l+1} = \xi_{i,l} - \sum_{j \in S_{i,k}} \delta(\xi_{i,l} - \xi_{j,l}), \quad l = 0, \ldots, r \quad (8)$$

$$\text{with} \quad \xi_{i,0} = \hat{x}_{i,k}, \quad i = 1 \ldots N, \quad (9)$$

$$s_{i,k} = \xi_{i,r}, \quad i = 1 \ldots N.$$

where r is the number of iterations per single time step, $\delta > 0$ is a design parameter, $S_{i,k}$ is the index set of neighbors for the agent i at time k, and $s_{i,k}$ is the current state estimate for ith agent. The gain matrices $L_{i,k}$ are computed by using the matrix L, which is defined as the *core* observer gain matrix corresponding to the core measurement z_k, as

$$L_{i,k} = L\left(E_{i,k}^T \text{diag}(h_{i,k})^{-1} \otimes I_p\right), \quad (10)$$

where $E_{i,k}$ and $h_{i,k}$ are as defined in (5) and (6). Since L is the observer gain for core measurements z_k, the actual measurements must be mapped back to the core measurements in order to apply the gain L. This mapping is done via the matrix $E_{i,k}^T \text{diag}(h_{i,k})^{-1} \otimes I_p$, by noting that

$$L_{i,k}y_{i,k} = L_{i,k}(E_{i,k} \otimes I_p)z_k = L(E_{i,k}^T \text{diag}(h_{i,k})^{-1} E_{i,k} \otimes I_p)Cx_k,$$

whose sum will lead to $L(\mathcal{L}(\mathbf{G}_{s,k}) \otimes I_p)Cx_k$ (see Eq. (6)). As will be shown in the proof of our first main result Theorem 1, this will then lead to agreement dynamics (will be defined later) whose stability is determined by the matrix $A + \frac{1}{N}L(\mathcal{L}(\mathbf{G}_{s,k}) \otimes I_p)C$. This is a time-varying matrix whose particular form is very conducive to our stability analysis.

The choices for the scalars r and δ and the synthesis of the gain matrix L will be explained in more detail later in the paper. Here we assume that the consensus filter can be iterated as many times as the integer r dictates during a single time step. Hence r is a design parameter determining the speed of the consensus dynamics for the stability of the observer. The design parameter δ can be selected as follows

$$0 < \delta < \frac{1}{\mathbf{d}(\mathbf{G}_{c,k})} \quad \forall\, k = 0, 1, \ldots. \quad (11)$$

This choice will be clarified in Theorem 1. Note that $\mathbf{d}(\mathbf{G}_{c,k}) \leq N - 1$ for an undirected graph with no multiple edges, and hence choosing $\delta \in (0, 1/(N-1))$ leads to the satisfaction of (11) for all communication graphs.

Intuitively, the observer can be explained as follows. First each agent collects all its available measurements and updates its observer state. Then it communicates its own state estimate to its neighbors while collecting and blending the neighbors' estimates with its own. The consensus filter only changes the observer states when there is a mismatch between them. If there were infinite number of consensus iterations and if the communication graph were connected, it is well known that this process would make each agent's observer estimate converge to a common value. Additionally, if the sensing graph is pseudo-connected, the set of all measurements has the information content of the core set. Since each agent has this information infused into its observer state via consensus and since (C, A) is detectable, it can be deduced that each agent's observer state will converge to the real state for large enough consensus iterations. However, this is practically infeasible. Since the main reason to use consensus is to eliminate a complicated measurement routing scheme through the communication network, using arbitrarily large number of consensus iterations will defeat this purpose. Hence we will find a safe upper bound on the number of consensus iterations to keep the observer exponentially stable.

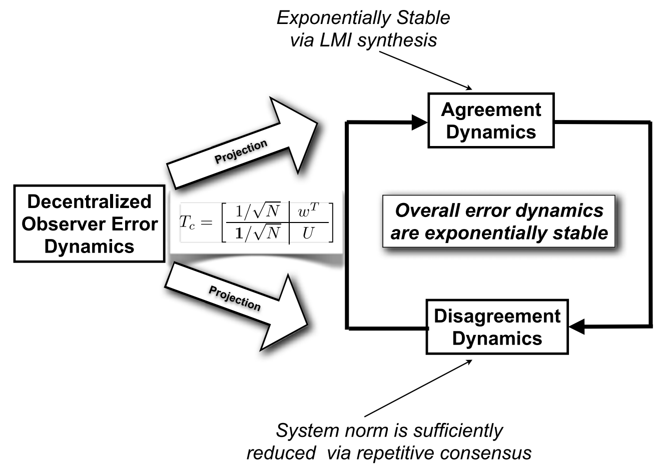

Fig. 1. Sketch of the proof of the exponential stability.

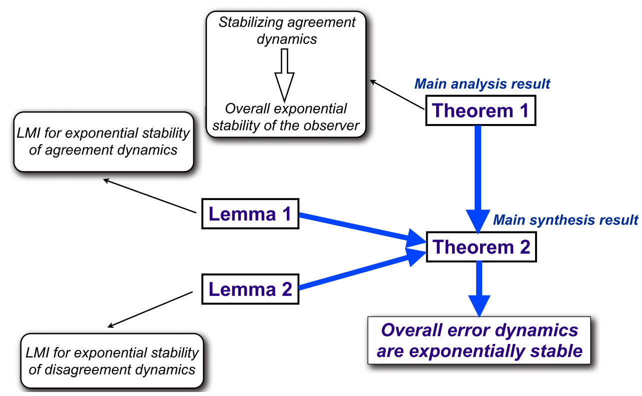

Fig. 2. Relationships between technical results: Theorem 1 is the main analysis result, which motivates the synthesis result given in Theorem 2. Lemmas 1 and 2 give LMI conditions for the exponential stability of the agreement and the disagreement dynamics. These LMI results are then used in Theorem 2, which combines them with Theorem 1 to obtain an LMI synthesis for the decentralized observer with an exponentially stable error dynamics.

3. Exponential stability of the decentralized observer

In this section, we present a constructive proof of the exponential stability of the decentralized observer. As depicted in Fig. 1, the observation error dynamics are projected into two subspaces: (i) agreement; (ii) disagreement subspaces. The main result of this section is Theorem 1 and it states that if agreement dynamics are exponentially stable then there is always a number of consensus updates that will ensure the exponential stability of the overall error dynamics. This result is key since it determines our synthesis strategy: (i) first the estimator gain is designed to guarantee exponential stability of the agreement dynamics (Section 4, Lemma 1); (ii) then a valid lower bound on the number of consensus iterations is computed to ensure the exponential stability of the overall error dynamics (Section 5, Theorem 2 that builds on Lemmas 1 and 2). See Fig. 2 for an overview of key results and their connections.

Let ξ_l be the overall (*augmented*) vector of $\xi_{i,l} \in \mathbb{R}^{nN}$ defined in (8) $\xi_l = (\xi_{1,l}, \xi_{2,l}, \ldots, \xi_{N,l})$. Similarly, we define $\hat{x}_k$, the augmented state estimate vector, and s_k (both in $\mathbb{R}^{nN}$), augmented state vector, as

$$\hat{x}_k := (\hat{x}_{1,k}, \hat{x}_{2,k}, \ldots, \hat{x}_{N,k}), \qquad s_k := (s_{1,k}, \ldots, s_{N,k}).$$

The ith row of the Laplacian matrix $\mathcal{L}(\mathbf{G}_{c,k})$ of the communication graph $\mathbf{G}_{c,k}$ at time k is formed such that the (i, i)th (diagonal) entry is the number of connections of the ith agent, and the (i, j)th entry is -1 if there is a connection between ith and jth agents and 0 otherwise. Consequently the overall consensus dynamics in (8) can be expressed as

$$\xi_{l+1} = (I_{nN} - \delta\mathcal{L}^{\otimes}_{c,k})\xi_l, \quad l = 0, \ldots, r, \text{ with } \xi_0 = \hat{x}_k,$$
$$\Rightarrow \xi_r = (I_{nN} - \delta\mathcal{L}^{\otimes}_{c,k})^r \hat{x}_k$$

where $\mathcal{L}^{\otimes}_{c,k} := \mathcal{L}(\mathbf{G}_{c,k}) \otimes I_n$. Let the observation error be defined as $e_{i,k} := \hat{x}_{i,k} - x_k$ and $e_k := (e_{1,k}, \ldots, e_{N,k})$, then using Eq. (7), can express the error dynamics as

$$\begin{aligned} e_{i,k+1} &= \hat{x}_{i,k+1} - x_{k+1} \\ &= As_{i,k} + L_{i,k}(C_{i,k}s_{i,k} - y_{i,k}) - Ax_k. \end{aligned}$$

Note that $s_{i,k}$ is the state estimate for ith agent. The above equation implies that

$$\begin{aligned} e_{k+1} &= A_{c,k}(s_k - \mathbf{1}_N \otimes x_k) \\ &= A_{c,k}(\xi_r - \mathbf{1}_N \otimes x_k) \\ &= A_{c,k}\left((I_{nN} - \delta\mathcal{L}^{\otimes}_{c,k})^r \hat{x}_k - \mathbf{1}_N \otimes x_k\right). \end{aligned} \tag{12}$$

where $A_{c,k}$ is defined as follows,

$$\begin{aligned} A_{c,k} &= \operatorname{diag}\left\{A + L_{i,k}C_{i,k};\ i = 1, \ldots, N\right\} \\ &= \operatorname{diag}\big\{A + L(E^T_{i,k}\operatorname{diag}(h_{i,k})^{-1}E_{i,k} \otimes I_p)C; \\ &\qquad i = 1, \ldots, N\big\}. \end{aligned} \tag{13}$$

Since $\mathcal{L}^{\otimes}_{c,k}(\mathbf{1}_N \otimes x_k) = (\mathcal{L}(\mathbf{G}_{c,k}) \otimes I_n)(\mathbf{1}_N \otimes x_k) = (\mathcal{L}(\mathbf{G}_{c,k})\mathbf{1}_N) \otimes x_k = 0$ and

$$(I_{nN} - \delta\mathcal{L}^{\otimes}_{c,k})^r = I_{nN} + (\ldots)\mathcal{L}^{\otimes}_{c,k} + (\ldots)\mathcal{L}^{\otimes^2}_{c,k} + \ldots,$$

the following identity follows

$$(\mathbf{1}_N \otimes x_k) = (I_{nN} - \delta\mathcal{L}^{\otimes}_{c,k})^r(\mathbf{1}_N \otimes x_k).$$

Substituting this identity in (12), we obtain

$$e_{k+1} = A_{c,k}(I_{nN} - \delta\mathcal{L}^{\otimes}_{c,k})^r \underbrace{\left(\hat{x}_k - \mathbf{1}_N \otimes x_k\right)}_{e_k}.$$

The above relationship implies that the overall error dynamics for e_k can be expressed in a compact form as

$$\begin{aligned} e_{k+1} &= A_{c,k}(I_{nN} - \delta\mathcal{L}^{\otimes}_{c,k})^r e_k \\ &= A_{c,k}[(I_N - \delta\mathcal{L}(\mathbf{G}_{c,k}))^r \otimes I_n]e_k. \end{aligned} \tag{14}$$

Eq. (14) is very useful since it describes the time evolution of the error vector, e_k, in a compact form that exposes the error dynamics as a function of three key parameters: (i) the observer gain L; (ii) the sensing graph represented by $E_{i,k}$; (iii) the communication graph represented by $\mathcal{L}(\mathbf{G}_{c,k})$.

The following theorem is our second key contribution that establishes conditions under which the observer error dynamics are exponentially stable.

Theorem 1. *Suppose that the sensing graph is pseudo-connected and communication graph is connected for all $k = 1, 2, \ldots$, and there exist some L, $P = P^T > 0$, and $\lambda \in [0, 1)$ such that the following inequality holds for the Laplacian, $\mathcal{L}_s$, of any pseudo-connected sensing graph $\mathbf{G}_s$,*

$$\lambda P - A_a(\mathcal{L}_s)^T P A_a(\mathcal{L}_s) \geq 0$$
$$\text{where } A_a(\mathcal{L}_s) := A + \frac{1}{N}L(\mathcal{L}_s \otimes I_p)C. \tag{15}$$

Let $\delta \in (0, 1/(N-1))$. Then there exists a large enough positive integer $r \geq 1$ such that the error dynamics of the observer given by Eq. (14) are globally exponentially stable (GES), hence the observer given by Eqs. (7) and (8) is GES and, for $i = 1, \ldots, N$,

$$\|\hat{x}_{i,k} - x_k\| \leq c_i\tilde{\lambda}_i^k\|\hat{x}_{i,0} - x_0\|, \quad \forall k = 0, 1, \ldots \tag{16}$$

for some $c_i > 0$ and $\tilde{\lambda}_i \in (0, 1)$.

Proof. The proof has the following main steps:

(1) Define a transformation projecting the error dynamics into agreement and disagreement dynamics, see Fig. 2.
(2) Proof of exponential stability of agreement dynamics via a quadratic Lyapunov function.
(3) Proof of the overall stability via a sufficient level of consensus with large enough r.

The first step is to find an appropriate transformation that will split the error vector e_k into *agreement* and *disagreement* subspaces. These subspaces bring a geometrical insight to the observer synthesis, and they help in clarifying the roles of the measurement and communication feedback terms in the observer. Consider the following "universal" transformation (time invariant and independent of both sensing and communication graphs),

$$T = \underbrace{\left[\begin{array}{c|ccccc} \frac{1}{\sqrt{N}} & \frac{1}{\sqrt{2}} & \frac{1}{\sqrt{6}} & \cdots & \frac{1}{\sqrt{N(N-1)}} \\ \hline & \frac{-1}{\sqrt{2}} & \frac{1}{\sqrt{6}} & \cdots & \frac{1}{\sqrt{N(N-1)}} \\ & 0 & \frac{-2}{\sqrt{6}} & \cdots & \frac{1}{\sqrt{N(N-1)}} \\ \frac{1}{\sqrt{N}} & \vdots & 0 & \ddots & \frac{1}{\sqrt{N(N-1)}} \\ & 0 & 0 & 0 & \frac{-(N-1)}{\sqrt{N(N-1)}} \end{array}\right]}_{T_c} \otimes I_n. \tag{17}$$

It can easily be shown that columns of T and T_c form an orthonormal set of vectors, hence T and T_c are orthogonal matrices such that $T^TT = TT^T = I_{nN}$ and $T_c^TT_c = T_cT_c^T = I_N$. Note that, for any graph without self loops or multiple edges $\mathbf{G}$, such as the communication graph, we have

$$\mathcal{L}(\mathbf{G}) = \left[\begin{array}{c|c} \mathbf{1}^T v & -v^T \\ \hline -v & V \end{array}\right] \tag{18}$$

for some vector $v \geq 0$ and matrix $V = V^T$, which are related by $V\mathbf{1} = v$, and we can express matrix T_c as follows,

$$T_c = \left[\begin{array}{c|c} 1/\sqrt{N} & w^T \\ \hline \mathbf{1}/\sqrt{N} & U \end{array}\right]$$

with appropriately defined vector w and matrix U. This implies that

$$T_c^T\mathcal{L}(\mathbf{G})T_c = \left[\begin{array}{c|c} 0 & \mathbf{0}^T \\ \hline \mathbf{0} & \mathcal{L}_p(\mathbf{G}) \end{array}\right], \tag{19}$$

where $\mathcal{L}_p(\mathbf{G}) \in \mathbb{R}^{(N-1)\times(N-1)}$ is a symmetric matrix given by

$$\mathcal{L}_p(\mathbf{G}) = (\mathbf{1}^T v)ww^T - wv^TU - U^Tvw^T + U^TVU. \tag{20}$$

This can be shown as follows:

$$T_c^T\mathcal{L}(\mathbf{G})T_c = \begin{bmatrix} \dfrac{1}{\sqrt{N}} & \dfrac{\mathbf{1}^T}{\sqrt{N}} \\ w & U^T \end{bmatrix}$$
$$\times \begin{bmatrix} \dfrac{1}{\sqrt{N}}(\underbrace{\mathbf{1}^Tv - v^T\mathbf{1}}_{0}) & \mathbf{1}^Tvw^T - v^TU \\ \underbrace{(-v + V\mathbf{1})}_{\mathbf{0}}/\sqrt{N} & -vw^T + VU \end{bmatrix}$$
$$= \begin{bmatrix} 0 & (\underbrace{\mathbf{1}^Tvw^T - \mathbf{1}^Tvw^T}_{\mathbf{0}^T}\underbrace{-v^TU + \overbrace{\mathbf{1}^TV}^{v^T}U}_{\mathbf{0}^T})/\sqrt{N} \\ \mathbf{0} & \mathcal{L}_p(\mathbf{G}) \end{bmatrix}.$$

Note that T_c (hence T) is a universal transformation that does not depend on the graph at hand, and it generates $\mathcal{L}_p(\mathbf{G})$ (that is a function of the graph), which is symmetric. Furthermore, since T_c is used as a similarity transformation, for any connected graph $\mathbf{G}$ without self-loops or multiple edges, $\sigma(\mathcal{L}(\mathbf{G})) = \sigma(T_c^T\mathcal{L}(\mathbf{G})T_c)$. This implies that

$$\sigma(\mathcal{L}_p(\mathbf{G})) = \sigma(\mathcal{L}(\mathbf{G})) \setminus \{0\} \subset [2(1-\cos(\pi/N)), 2\mathbf{d}(\mathbf{G})]. \tag{21}$$

Define the transformed error as,

$$\tilde{e}_k \triangleq T^T e_k. \tag{22}$$

Then Eq. (14) can be written as,

$$\begin{aligned}\tilde{e}_{k+1} &= T^T A_{c,k}[(I_N - \delta\mathcal{L}(\mathbf{G}_{c,k}))^r \otimes I_n]T\tilde{e}_k \\ &= \underbrace{T^T A_{c,k} T}_{:=\tilde{A}_{c,k}} \; \underbrace{T^T[(I_N - \delta\mathcal{L}(\mathbf{G}_{c,k}))^r \otimes I_n]T}_{:=\Lambda_k^r \otimes I_n}\,\tilde{e}_k.\end{aligned} \tag{23}$$

Next we derive an expression for Λ_k. Noting that $T = T_c \otimes I_n$ and $(Z_1 \otimes Z_2)(Z_3 \otimes Z_4) = (Z_1Z_3) \otimes (Z_2Z_4)$ for compatible matrices $Z_1, \ldots, Z_4$, we have

$$\begin{aligned}&T^T[(I_N - \delta\mathcal{L}(\mathbf{G}_{c,k}))^r \otimes I_n]T \\ &\quad= (T_c \otimes I_n)^T[(I_N - \delta\mathcal{L}(\mathbf{G}_{c,k}))^r \otimes I_n](T_c \otimes I_n) \\ &\quad= (T_c \otimes I_n)^T[(I_N - \delta\mathcal{L}(\mathbf{G}_{c,k}))^r T_c \otimes I_n] \\ &\quad= \underbrace{[T_c^T(I_N - \delta\mathcal{L}(\mathbf{G}_{c,k}))^r T_c]}_{=\Lambda_k^r} \otimes I_n,\end{aligned}$$

which implies that $\Lambda_k = T_c^T(I_N - \delta\mathcal{L}(\mathbf{G}_{c,k}))T_c$. By noting $(I_N - \delta\mathcal{L}(\mathbf{G}_{c,k}))^r = I_N + c_1\mathcal{L}(\mathbf{G}_{c,k}) + c_2\mathcal{L}(\mathbf{G}_{c,k})^2 + \cdots + c_r\mathcal{L}(\mathbf{G}_{c,k})^r$ for some $c_1, \ldots, c_r \in \mathbb{R}$, we have

$$\begin{aligned}\Lambda_k^r &= T_c^T(I_N - \delta\mathcal{L}(\mathbf{G}_{c,k}))^r T_c \\ &= T_c^T I_N T_c + c_1 T_c^T\mathcal{L}(\mathbf{G}_{c,k})T_c + c_2 T_c^T\mathcal{L}(\mathbf{G}_{c,k})^2 T_c + \cdots \\ &\quad + c_r T_c^T\mathcal{L}(\mathbf{G}_{c,k})^r T_c \\ &= I_N + c_1\tilde{\mathcal{L}}_{c,k} + c_2\tilde{\mathcal{L}}_{c,k}^2 + \cdots c_r\tilde{\mathcal{L}}_{c,k}^r = (I_N - \delta\tilde{\mathcal{L}}_{c,k})^r.\end{aligned}$$

The newly defined $\tilde{\mathcal{L}}_{c,k}$ is given by

$$\tilde{\mathcal{L}}_{c,k} \triangleq T_c^T\mathcal{L}(\mathbf{G}_{c,k})T_c = \begin{bmatrix} 0 & \mathbf{0}^T \\ \mathbf{0} & \mathcal{L}_p(\mathbf{G}_{c,k}) \end{bmatrix},$$

which is obtained by noting that the first column of T_c, $\mathbf{1}$, is in the null space of $\mathcal{L}(\mathbf{G}_{c,k})$, that is, $\mathcal{L}(\mathbf{G}_{c,k})\mathbf{1} = \mathbf{0}$. Consequently

$$\begin{aligned}\Lambda_k^r &= (I_N - \delta\tilde{\mathcal{L}}_{c,k})^r = \left(\begin{bmatrix} 1 & \mathbf{0}^T \\ \mathbf{0} & I_{N-1} \end{bmatrix} - \delta\begin{bmatrix} 0 & \mathbf{0}^T \\ \mathbf{0} & \mathcal{L}_p(\mathbf{G}_{c,k}) \end{bmatrix}\right)^r \\ &= \begin{bmatrix} 1 & \mathbf{0}^T \\ \mathbf{0} & I_{N-1} - \delta\mathcal{L}_p(\mathbf{G}_{c,k}) \end{bmatrix}^r.\end{aligned}$$

This transformation allows us to project the overall estimation error vector $\tilde{e}_k$ into its components in the *agreement* subspace, ε_k, and the *disagreement* subspace, η_k,

$$\begin{aligned}\tilde{e}_{k+1} &= \begin{bmatrix} \varepsilon_{k+1} \\ \eta_{k+1} \end{bmatrix} = A_e \begin{bmatrix} \varepsilon_k \\ \eta_k \end{bmatrix} \\ &\text{where } A_e = \begin{bmatrix} A_a(\mathbf{G}_{s,k}) & F_k\Lambda_{p,k}^r \\ G_k & A_{d,k}\Lambda_{p,k}^r \end{bmatrix},\end{aligned} \tag{24}$$

and

$$A_a(\mathbf{G}_{s,k}) = A + \frac{1}{N}L\underbrace{\left(\sum_{i=1}^{N} E_{i,k}^T \mathrm{diag}(h_{i,k})^{-1}E_{i,k} \otimes I_p\right)}_{\mathcal{L}(\mathbf{G}_{s,k})\otimes I_p} C,$$

$$\Lambda_{p,k} = (I_{N-1} - \delta\mathcal{L}_p(\mathbf{G}_{c,k})) \otimes I_n,$$

$$G_k = \begin{bmatrix} \dfrac{L_{1,k}C_{1,k} - L_{2,k}C_{2,k}}{\sqrt{2N}} \\ \dfrac{L_{1,k}C_{1,k} + L_{2,k}C_{2,k} - 2L_{3,k}C_{3,k}}{\sqrt{6N}} \\ \vdots \\ \dfrac{\sum_{i=1}^{N-1} L_{i,k}C_{i,k} - (N-1)L_{N,k}C_{N,k}}{\sqrt{N^2(N-1)}} \end{bmatrix},$$

$$F_k = \left[\frac{L_{1,k}C_{1,k} - L_{2,k}C_{2,k}}{\sqrt{2N}}\; \frac{L_{1,k}C_{1,k} + L_{2,k}C_{2,k} - 2L_{3,k}C_{3,k}}{\sqrt{6N}}, \ldots \right. \\ \left. \frac{\sum_{i=1}^{N-1} L_{i,k}C_{i,k} - (N-1)L_{N,k}C_{N,k}}{\sqrt{N^2(N-1)}}\right].$$

The terms in Eq. (24), $A_a(\mathbf{G}_{s,k})$, G_k, and F_k are shown to be as above by simply substituting Eqs. (13) and (17) in Eq. (23). Since their derivations are straightforward algebraic manipulations, which do not add any further insight to the discussion, they are omitted. We also do not need the explicit form of $A_{d,k}$ (defined in (24)) in the proof. $\mathcal{L}_p(\mathbf{G}_{c,k})$, (2, 2) block of the matrix $(T_c^T\mathcal{L}(\mathbf{G}_{c,k})T_c)$, is a symmetric matrix with $2(1-\cos(\pi/N))I \le \mathcal{L}_p(\mathbf{G}_{c,k}) \le 2\mathbf{d}(\mathbf{G}_{c,k})I$. Hence the choice of $\delta \in (0, 1/(N-1))$ renders the eigenvalues of the Laplacian of any connected communication graph inside the unit circle, i.e., $\rho(\Lambda_{p,k}) < 1$ (see Eq. (11)).

With the transformed state we can express the Lyapunov function as follows:

$$\tilde{V}(\tilde{e}_k) = \tilde{e}_k^T(I_\alpha^{-1} \otimes P)\tilde{e}_k, \quad \text{where } I_\alpha = \begin{bmatrix} 1 & 0 \\ 0 & \alpha I_{N-1} \end{bmatrix}$$

and $\alpha > 0$.

Consider some $\gamma \in (\lambda, 1)$, we have

$$\begin{aligned}&\gamma\tilde{V}(\tilde{e}_k) - \tilde{V}(\tilde{e}_{k+1}) = \tilde{e}_k^T S\,\tilde{e}_k, \\ &\text{where } S := \gamma(I_\alpha^{-1} \otimes P) - A_e^T(I_\alpha^{-1} \otimes P)A_e.\end{aligned} \tag{25}$$

We can express the matrix S as

$$\begin{aligned}S &= \begin{bmatrix} \gamma P & 0 \\ 0 & \gamma(\alpha^{-1}I_{N-1} \otimes P) \end{bmatrix} \\ &\quad - \begin{bmatrix} A_a(\mathbf{G}_{s,k}) & F_k\Lambda_{p,k}^r \\ G_k & A_{d,k}\Lambda_{p,k}^r \end{bmatrix}^T \begin{bmatrix} P & 0 \\ 0 & \alpha^{-1}I_{N-1} \otimes P \end{bmatrix} \\ &\quad \times \begin{bmatrix} A_a(\mathbf{G}_{s,k}) & F_k\Lambda_{p,k}^r \\ G_k & A_{d,k}\Lambda_{p,k}^r \end{bmatrix} \\ &= S_1 - S_2,\end{aligned}$$

where S_1 and S_2 are symmetric matrices defined by

$$S_1 = \begin{bmatrix} \gamma P - A_a(\mathbf{G}_{s,k})^T P A_a(\mathbf{G}_{s,k}) - \alpha^{-1} G_k^T \hat{P} G_k & 0 \\ 0 & \alpha^{-1}\gamma \hat{P} \end{bmatrix},$$

$$S_2 = \begin{bmatrix} 0 & \alpha^{-1} G_k^T \hat{P} A_{d,k} \Lambda_{p,k}^r + A_a(\mathbf{G}_{s,k})^T P F_k \Lambda_{p,k}^r \\ (\star)^T & \Lambda_{p,k}^r (\alpha^{-1} A_{d,k}^T \hat{P} A_{d,k} + F_k^T P F_k) \Lambda_{p,k}^r \end{bmatrix},$$

with $\hat{P} = I_{N-1} \otimes P$. By using the inequality (15), for any k,

$$\gamma P - A_a(\mathbf{G}_{s,k})^T P A_a(\mathbf{G}_{s,k}) = \underbrace{\lambda P - A_a(\mathbf{G}_{s,k})^T P A_a(\mathbf{G}_{s,k})}_{\geq 0} + (\gamma - \lambda) P$$

$$\Rightarrow \gamma P - A_a(\mathbf{G}_{s,k})^T P A_a(\mathbf{G}_{s,k}) \geq (\gamma - \lambda) P > 0.$$

This implies that agreement dynamics exponentially stable (dynamics with $\eta_k = 0$). Moreover $\alpha > 0$ can be chosen large enough such that $S_1 = S_1^T > 0$.

Next observe that $\Lambda_{p,k}$ is a symmetric matrix with all its eigenvalues in $(\lambda_{\min}, \lambda_{\max}) \subset (-1, 1)$. Hence $\lim_{r\to\infty} \lambda_{\min}^r I \leq \lim_{r\to\infty} \Lambda_{p,k}^r \leq \lim_{r\to\infty} \lambda_{\max}^r I = 0$. Since all nonzero blocks of S_2 contain $\Lambda_{p,k}^r$ as common factor, $\lim_{r\to\infty} S_2 = 0$. This implies that the spectral radius of the symmetric matrix $S_2 = S_2^T$ can be made arbitrarily small by choosing r large enough for a given α. Consequently, since $S_1 = S_1^T > 0$ by a choice of a large enough α, we can guarantee that $S = S_1 - S_2 > 0$ by choosing r large enough. This then implies that

$$\gamma \tilde{V}(\tilde{e}_k) - \tilde{V}(\tilde{e}_{k+1}) = \tilde{e}_k^T S \tilde{e}_k \geq \tilde{\lambda} \tilde{V}(\tilde{e}_k) > 0 \quad \text{for } \tilde{e}_k \neq 0,$$

for some $\tilde{\lambda} \in (0, 1)$. Since $\tilde{V}$ is positive definite quadratic function of $\tilde{e}_k$. This implies the exponential stability of the error dynamics. Eq. (16) is a direct consequence of this exponential stability, which concludes the proof. ■

4. LMI synthesis of exponentially stable agreement dynamics

This section will construct an LMI procedure to synthesize the gain matrix L to quadratically stabilize the agreement subspace of the error dynamics. Note that Eq. (24) implies that the error in the agreement subspace evolves, when $\eta_k = 0$, as follows,

$$\varepsilon_{k+1} = A_a(\mathbf{G}_{s,k}) \varepsilon_k.$$

As an immediate consequence of this observation, the condition (15) to hold for any pseudo-connected sensing graph implies that the error dynamics are quadratically stable in the agreement subspace.

Next we will construct the quadratic Lyapunov function of the condition (15). Since the sensing graph $\mathbf{G}_{s,k}$ is assumed to be pseudo connected, by using Theorem 3 together with Eqs. (48) and (49) in the Appendix, we have

$$2\left(1 - \cos\frac{\pi}{2N+1}\right) I \leq \sum_{i=1}^{N} E_{i,k}^T \operatorname{diag}(h_{i,k})^{-1} E_{i,k}$$
$$= \mathcal{L}(\mathbf{G}_{s,k}) \leq \left(2\mathbf{d}\left(\mathbf{G}_{s_k}^o\right) + 1\right) I, \tag{26}$$

where $\mathbf{G}_{s_k}^o$ is the sensing graph with the self-loops removed. Note that, since $\mathbf{G}_{s,k}$ has m vertices, $\mathbf{d}(\mathbf{G}_{s_k}^o) \leq m - 1$. Let

$$\beta_1 = 2\left(1 - \cos\frac{\pi}{2N+1}\right),$$
$$\beta_2 = \max_k 2\mathbf{d}(\mathbf{G}_{s_k}^o) + 1 \leq 2m - 1.$$

Now we can express the matrix $A_a(\mathbf{G}_{s,k})$ defined in Eq. (15) for each time instance k as follows

$$\begin{aligned} A_a(\mathbf{G}_{s,k}) &= A + \frac{1}{N} L \left(\mathcal{L}(\mathbf{G}_{s,k}) \otimes I_p\right) C \\ &\quad + \frac{\beta_1 + \beta_2}{2N} LC - \frac{\beta_1 + \beta_2}{2N} LC \\ &= A + \frac{1}{N} L \underbrace{\left(\mathcal{L}(\mathbf{G}_{s,k}) \otimes I_p - \frac{\beta_1 + \beta_2}{2} I\right)}_{\Delta_k} C + \frac{\beta_1 + \beta_2}{2N} LC \\ &= A + \frac{\beta_1 + \beta_2}{2N} LC + \frac{1}{N} L \Delta_k C \end{aligned}$$

where $-\frac{\beta_2 - \beta_1}{2} I \leq \Delta_k \leq \frac{\beta_2 - \beta_1}{2} I$. Then the *agreement dynamics* for ε_k, when $\eta_k = 0$ for all k, are given by:

$$\boxed{\begin{aligned} \epsilon_{k+1} &= \underbrace{\left(A + \frac{\beta_1 + \beta_2}{2N} LC\right)}_{:= A_\epsilon} \epsilon_k + \frac{1}{N} L p_k \\ p_k &= \Delta_k q_k, \quad q_k = C \epsilon_k, \quad -\tilde{\beta} I \leq \Delta_k = \Delta_k^T \leq \tilde{\beta} I \end{aligned}} \tag{27}$$

where $\tilde{\beta} = \frac{\beta_2 - \beta_1}{2} > 0$. We will establish the quadratic stability of the above system via a choice of the gain matrix L. The agreement dynamics given by (27) above, is known in the Norm-Bound Linear Differential Inclusion (NLDI) (Boyd et al., 1994) form. Note that,

$$p_k = \Delta_k q_k, \quad \|\Delta_k\| \leq \tilde{\beta} \Leftrightarrow p_k^T p_k \leq \tilde{\beta}^2 q_k^T q_k. \tag{28}$$

The expression (28) can be rewritten as,

$$\begin{bmatrix} q_k \\ p_k \end{bmatrix}^T M \begin{bmatrix} q_k \\ p_k \end{bmatrix} \geq 0 \quad \text{where } M = \begin{bmatrix} \hat{\alpha}\tilde{\beta}^2 I & 0 \\ 0 & -\hat{\alpha} I \end{bmatrix} \tag{29}$$

where $\hat{\alpha} > 0$ is a scalar variable introduced through S-procedure (Açıkmeşe & Corless, 2008; Boyd et al., 1994).

Lemma 1. *Consider the agreement dynamics given by* (27) *with the gain matrix L given by $L = P^{-1}S$, where $P = P^T > 0$ and S are obtained jointly by solving the following ADLMI (Agreement Dynamics LMI) for some $\lambda \in [0, 1)$, with solution variables P, S, and $\hat{\alpha}$,*

$$\begin{bmatrix} \lambda P - \hat{\alpha}\tilde{\beta}^2 C^T C & 0 & A^T P + \frac{\beta_1 + \beta_2}{2N} C^T S^T \\ 0 & \hat{\alpha} I & \frac{1}{N} S^T \\ PA + \frac{\beta_1 + \beta_2}{2N} SC & \frac{1}{N} S & P \end{bmatrix} \geq 0. \tag{30}$$

Then the resulting agreement dynamics (27) *are quadratically (hence globally exponentially) stable, and the condition* (15) *in* Theorem 1 *is satisfied with L, P, and λ.*

Proof. Consider a Lyapunov function $V(\varepsilon_k) = \varepsilon_k^T P \varepsilon_k$ with $P = P^T > 0$ such that, for some $\lambda \in (0, 1)$,

$$\lambda V_k - V_{k+1} \geq 0, \quad \forall \begin{bmatrix} q_k \\ p_k \end{bmatrix}^T M \begin{bmatrix} q_k \\ p_k \end{bmatrix} \geq 0. \tag{31}$$

We combine the two inequalities in (31) into the following inequality via the S-procedure (Boyd et al., 1994) by noting that any positive multiple of a multiplier matrix M is also a multiplier

$$\lambda V_k - V_{k+1} - \begin{bmatrix} q_k \\ p_k \end{bmatrix}^T M \begin{bmatrix} q_k \\ p_k \end{bmatrix} \geq 0,$$

for all $\varepsilon_k,\ q_k,\ p_k$. Then the above inequality implies that

$$\lambda \varepsilon_k^T P \varepsilon_k - \left(A_\varepsilon \varepsilon_k + \frac{1}{N} L p_k\right)^T P \left(A_\varepsilon \varepsilon_k + \frac{1}{N} L p_k\right) - \begin{bmatrix} \varepsilon_k \\ p_k \end{bmatrix}^T \begin{bmatrix} C & 0 \\ 0 & I \end{bmatrix}^T M \begin{bmatrix} C & 0 \\ 0 & I \end{bmatrix} \begin{bmatrix} \varepsilon_k \\ p_k \end{bmatrix} \geq 0.$$

The above inequality is equivalent to

$$\begin{bmatrix} \lambda P - A_\varepsilon^T P A_\varepsilon - \hat{\alpha} \tilde{\beta}^2 C^T C & -\frac{1}{N} A_\varepsilon^T P L \\ -\frac{1}{N} L^T P A_\varepsilon & \hat{\alpha} I - \frac{1}{N^2} L^T P L \end{bmatrix} \geq 0$$

$$\Rightarrow \begin{bmatrix} \lambda P - \hat{\alpha} \tilde{\beta}^2 C^T C & 0 \\ 0 & \hat{\alpha} I \end{bmatrix} - \underbrace{\begin{bmatrix} A_\varepsilon^T P A_\varepsilon & \frac{1}{N} A_\varepsilon^T P L \\ \frac{1}{N} L^T P A_\varepsilon & \frac{1}{N^2} L^T P L \end{bmatrix}}_{G} \geq 0,$$

$$\text{where } G = \begin{bmatrix} A_\varepsilon^T P \\ \frac{1}{N} L^T P \end{bmatrix} P^{-1} \begin{bmatrix} P A_\varepsilon & \frac{1}{N} P L \end{bmatrix}.$$

Using the Schur complements (Boyd et al., 1994), this is equivalent to

$$\begin{bmatrix} \lambda P - \hat{\alpha} \tilde{\beta}^2 C^T C & 0 & A_\varepsilon^T P \\ 0 & \hat{\alpha} I & \frac{1}{N} L^T P \\ P A_\varepsilon & \frac{1}{N} P L & P \end{bmatrix} \geq 0$$

with $P = P^T > 0,\ \hat{\alpha} > 0$.

Finally, by setting $S = PL$ and by expanding A_ε, the ADLMI feasibility problem is obtained with the solution variables S, P, and $\hat{\alpha}$. This shows that the satisfaction of ADLMI implies the existence of a quadratic Lyapunov function proving the quadratic stability of the agreement dynamics, and furthermore this Lyapunov function satisfies the condition (15). Note that, once a feasible solution of the above ADLMI is obtained, we can construct the gain matrix by using $L = P^{-1} S$, that is, the observer gain matrix L is synthesized by solving for $P = P^T > 0$ satisfying the ADLMI (30). ■

5. Bound on consensus iterations for observer stability

Next, we compute a bound on the number of iterations, r, to ensure exponential stability of the overall error dynamics. As shown in Eq. (43), the bound on r will depend on the bound of P-norm of $A_{i,k} := A + L_{i,k} C_{i,k}$ as in Eq. (13), that is,

$$A_{i,k} = A + L(E_{i,k}^T \operatorname{diag}(h_{i,k})^{-1} E_{i,k} \otimes I_p). \tag{32}$$

In this section, we establish this bound, $\bar{a}$, that is, $\|A_{i,k}\|_P \leq \bar{a}$ for all i and k and for all indices i and k,

$$\|A_{i,k}\|_P \leq \bar{a} \iff w^T A_{i,k}^T P A_{i,k} w \leq \bar{a}^2 w^T P w \quad \forall w. \tag{33}$$

Since $A_{i,k}$ does not necessarily have all its eigenvalues in the unit circle, due to lack of detectability with local measurements, a part of the error may grow. We bound the growth of the local observation error after the measurement update.

Lemma 2. *Given $A_{i,k}$ as in Eq. (32), then $\|A_{i,k}\|_P \leq \bar{a}$ for all $i,\ k$ if the following matrix inequality is satisfied for some $\tilde{\alpha} > 0$,*

$$\begin{bmatrix} \bar{a}^2 P - A^T P A & -A^T S - \tilde{\alpha} \beta_2 C^T & 0 \\ -SA - \tilde{\alpha} \beta_2 C & 2\tilde{\alpha} I & S^T \\ 0 & S & P \end{bmatrix} \geq 0, \tag{34}$$

where $\beta_2 = \max_k 2\mathbf{d}(\mathbf{G}_{s,k}^o) + 1 (\leq 2m - 1)$.

Proof. The inequality (33) indicates that, to prove $\|A_{i,k}\|_P \leq \bar{a}$ is equivalent to proving that $\bar{a}^2 V_k - V_{k+1} \geq 0$ for $V_k = w_k^T P w_k$ and w_k is the state of the following system

$$w_{k+1} = A_{i,k} w_k.$$

This discrete-time system can be rewritten in an LDI form as

$$w_{k+1} = A w_k + L \tilde{p}_k, \quad \tilde{p}_k = \Omega_{i,k} \tilde{q}_k,\ \tilde{q}_k = C w_k,$$

where $\Omega_{i,k} = E_{i,k}^T \operatorname{diag}(h_{i,k})^{-1} E_{i,k}$. Noting that $0 \leq \Omega_{i,k} \leq \beta_2 I$, we define the following multiplier matrices for this system

$$M = \begin{bmatrix} 0 & \tilde{\alpha} \beta_2 I \\ \tilde{\alpha} \beta_2 I & -2\tilde{\alpha} I \end{bmatrix}.$$

This implies that $[\tilde{q}_k^T,\ \tilde{p}_k^T] M [\tilde{q}_k^T,\ \tilde{p}_k^T]^T \geq 0$ for all k. Then satisfaction of the following inequality implies that $\bar{a}^2 V_k - V_{k+1} \geq 0$ for all w_k, and hence $\|A_{i,k}\|_P \leq \bar{a}$,

$$\bar{a}^2 V_k - V_{k+1} - \begin{bmatrix} \tilde{q}_k \\ \tilde{p}_k \end{bmatrix}^T M \begin{bmatrix} \tilde{q}_k \\ \tilde{p}_k \end{bmatrix} \geq 0, \quad \tilde{q}_k = C w_k,\ \forall w_k,\ \tilde{p}_k.$$

The above inequality is equivalent to

$$\begin{bmatrix} \bar{a}^2 P - A^T P A & -A^T P L - \tilde{a} \beta_2 C^T \\ -L^T P A - \tilde{a} \beta_2 C & 2\tilde{a} I - L^T P L \end{bmatrix} \geq 0,$$

which is then equivalent to

$$\begin{bmatrix} \bar{a}^2 P - A^T P A & -A^T P L - \tilde{a} \beta_2 C^T \\ -L^T P A - \tilde{a} \beta_2 C & 2\tilde{a} I \end{bmatrix} - \begin{bmatrix} 0 \\ L^T P \end{bmatrix} P^{-1} \begin{bmatrix} 0 \\ L^T P \end{bmatrix}^T \geq 0.$$

By using the Schur complements and letting $S = PL$, we now obtain the desired matrix inequality (34). ■

We now present the key synthesis result of this paper, Theorem 2, to compute a bound on the number of consensus iterations r needed for an exponentially stable decentralized observer. To do that, the error dynamics (14) and the transformed error dynamics (23) are utilized,

$$e_{k+1} = A_{c,k} (I_{nN} - \delta \mathcal{L}_{c,k}^{\otimes})^r e_k \Rightarrow \tilde{e}_{k+1} = \tilde{A}_{c,k} (\Lambda_k^r \otimes I) \tilde{e}_k$$

where $\tilde{e}_k = T^T e_k$, and $\tilde{A}_{c,k}$ and Λ_k are defined in Eq. (23). A new quantity θ is defined that is instrumental in Theorem 2: a bound on the norm of matrix $\|\Lambda_{p,k}\| \leq \theta$, where $\Lambda_{p,k} = (I_{N-1} - \delta \mathcal{L}_p(\mathbf{G}_{c,k})) \otimes I_n$ with $\mathcal{L}_p$ as defined in (20). A simple optimization problem is constructed to compute a nonconservative value for θ. Let $\underline{b}$ and $\bar{b}$ be the lower and upper bounds on $\mathcal{L}_p(\mathbf{G}_{c,k})$, as defined in Eqs. (48) and (49), respectively

$$\underline{b} := \min_{k=0,1,\ldots} \mathbf{a}(\mathbf{G}_{c,k}) \geq 2(1 - \cos(\pi/N)) \quad \text{and}$$
$$\bar{b} := \max_{k=0,1,\ldots} \rho(\mathcal{L}(\mathbf{G}_{c,k})) \leq 2(N-1). \tag{35}$$

Note that the right-hand side of the inequalities provide analytical bounds on $\underline{b}$ and $\bar{b}$, which can be made tighter if the communication graphs had more specific structures that can be exploited, as will be discussed in detail in Section 6. Next we define θ as

$$\theta = \min_{\delta > 0} \max \left\{ |1 - \delta \bar{b}|,\ |1 - \delta \underline{b}| \right\}. \tag{36}$$

A byproduct of the solution of (36) is the optimal value of δ, which determines the value of δ used in the consensus part of the observer in (8):

$$\delta_* = \arg\min_{\delta>0} \max\left\{|1-\delta\bar{b}|, |1-\delta\underline{b}|\right\}. \tag{37}$$

A simple line search over δ can be performed to solve the optimization problem (36). Note that $\theta \in [0, 1)$. $\theta \geq 0$ is a direct implication of the definition. Since $\bar{b} \geq \underline{b} > 0$, setting $\delta = 1/\underline{b}$ implies that $\max\left\{|1-\delta\bar{b}|, |1-\delta\underline{b}|\right\} = 1-\underline{b}/\bar{b} < 1$, which then implies that $\theta < 1$.

The following theorem is our third main contribution, which establishes a general bound on the number of consensus iterations needed for the exponential stability of the error dynamics, in terms of the properties of the system dynamics and the sensing and the communication graphs.

Theorem 2. *Suppose that there exist $\hat{\alpha} > 0$, $\tilde{\alpha} > 0$, $P = P^T > 0$, and S such that the matrix inequalities (30) and (34) are satisfied for some $\lambda \in [0, 1)$ and $\bar{a} > 0$. Then the overall error dynamics given by (14) are exponentially stable if the integer $r \geq 1$ is chosen such that $\rho(\Gamma(r)) < 1$, where*

$$\Gamma(r) = \begin{bmatrix} \sqrt{\lambda} & \bar{a}\theta^r \\ \bar{a} & \bar{a}\theta^r \end{bmatrix} \quad \text{and } \theta \in [0, 1) \text{ is given by (36).} \tag{38}$$

Proof. For any vector ϕ of appropriate dimension, we have $\|\tilde{A}_{c,k}\phi\|_{I_N\otimes P} \leq \|\tilde{A}_{c,k}\|_{I_N\otimes P}\|\phi\|_{I_N\otimes P}$. The P-norm of $\tilde{A}_{c,k}$ can be simplified,

$$\begin{aligned}\|\tilde{A}_{c,k}\|_{I_N\otimes P} &= \left\|\left(I_N\otimes P^{\frac{1}{2}}\right)(T_c^T\otimes I_n)A_{c,k}(T_c\otimes I_n)\left(I_N\otimes P^{-\frac{1}{2}}\right)\right\| \\ &= \left\|(T_c^T\otimes I_n)\left(I_N\otimes P^{\frac{1}{2}}\right)A_{c,k}\left(I_N\otimes P^{-\frac{1}{2}}\right)(T_c\otimes I_n)\right\| \\ &= \|A_{c,k}\|_{I_N\otimes P},\end{aligned}$$

where we use that $T_cT_c^T = T_c^TT_c = I$ and $\|T_c\| = 1$ (see Eq. (17) for T_c). Then we can infer the following expression,

$$\begin{aligned}\|\tilde{e}_{k+1}\|_{I_N\otimes P} &\leq \|\tilde{A}_{c,k}\|_{I_N\otimes P}\|\underbrace{(\Lambda_k^r\otimes I)\tilde{e}_k}_{\phi_k}\|_{I_N\otimes P} \\ &= \|A_{c,k}\|_{I_N\otimes P}\|\phi_k\|_{I_N\otimes P}.\end{aligned}$$

Then, by using Eq. (24) we have

$$\|\eta_{k+1}\|_{I_{N-1}\otimes P} \leq \|\tilde{e}_{k+1}\|_{I_N\otimes P} \leq \|A_{c,k}\|_{I_N\otimes P}\|\phi_k\|_{I_N\otimes P}. \tag{39}$$

Here, ϕ_k can be represented as

$$\phi_k = \begin{bmatrix}\varepsilon_k \\ \Lambda_{p,k}^r\eta_k\end{bmatrix} \Rightarrow \|\phi_k\|_{I_N\otimes P} \leq \|\varepsilon_k\|_P + \|\Lambda_{p,k}^r\eta_k\|_{I_{N-1}\otimes P},$$

with $\Lambda_{p,k}$ defined from Eq. (24) as $\Lambda_{p,k} = (I_{N-1} - \delta\mathcal{L}_p(\mathbf{G}_{c,k}))\otimes I_n$. From here,

$$\|\Lambda_{p,k}^r\eta_k\|_{I_{N-1}\otimes P} \leq \|\Lambda_{p,k}^r\|_{I_{N-1}\otimes P}\|\eta_k\|_{I_{N-1}\otimes P}.$$

Now we have,

$$\begin{aligned}\|\Lambda_{p,k}\|_{I_{N-1}\otimes P} &= \left\|\left(I_{N-1}\otimes P^{\frac{1}{2}}\right)\Lambda_{p,k}\left(I_{N-1}\otimes P^{-\frac{1}{2}}\right)\right\| \\ &= \left\|\left(I_{N-1}\otimes P^{\frac{1}{2}}\right)(I_{N-1}-\delta\mathcal{L}_p(\mathbf{G}_{c,k})) \right. \\ &\quad \left. \otimes I_n\left(I_{N-1}\otimes P^{-\frac{1}{2}}\right)\right\| \\ &= \|(I_{N-1}-\delta\mathcal{L}_p(\mathbf{G}_{c,k}))\otimes I_n\| = \|\Lambda_{p,k}\|.\end{aligned}$$

This implies that,

$$\begin{aligned}\|\Lambda_{p,k}^r\eta_k\|_{I_{N-1}\otimes P} &\leq \|\Lambda_{p,k}\|_{I_{N-1}\otimes P}\|\Lambda_{p,k}^{r-1}\eta_k\|_{I_{N-1}\otimes P} \\ &= \|\Lambda_{p,k}\|\,\|\Lambda_{p,k}^{r-1}\eta_k\|_{I_{N-1}\otimes P} \\ &\;\;\vdots \\ &\leq \|\Lambda_{p,k}\|^r\|\eta_k\|_{I_{N-1}\otimes P} \leq \theta^r\|\eta_k\|_{I_{N-1}\otimes P},\end{aligned}$$

where $\theta \geq \|\Lambda_{p,k}\|\forall k$. Then, by letting $\bar{a}$ such that $\|A_{c,k}\|_{I_N\otimes P} \leq \bar{a}$, and combining these results with Eq. (39) we get:

$$\|\eta_{k+1}\|_{I_{N-1}\otimes P} \leq \bar{a}\|\varepsilon_k\|_P + \bar{a}\theta^r\|\eta_k\|_{I_{N-1}\otimes P}. \tag{40}$$

Again by using Eq. (24), $\|A_a(\mathbf{G}_{s,k})\varepsilon_k\|_p \leq \sqrt{\lambda}\|\varepsilon_k\|_P$, and the triangle inequality with P-norm,

$$\|\varepsilon_{k+1}\|_P \leq \sqrt{\lambda}\|\varepsilon_k\|_P + \|F_k\Lambda_{p,k}^r\eta_k\|_p, \tag{41}$$

where

$$\begin{aligned}\|F_k\Lambda_{p,k}^r\eta_k\|_P &= \left\|\begin{bmatrix}F_k\Lambda_{p,k}^r\eta_k \\ \mathbf{0}\end{bmatrix}\right\|_{I_N\otimes P} \\ &= \left\|\begin{bmatrix}\mathbf{0} & F_k \\ \mathbf{0} & \mathbf{0}\end{bmatrix}\begin{bmatrix}\mathbf{0} \\ \Lambda_{p,k}^r\eta_k\end{bmatrix}\right\|_{I_N\otimes P} \\ &\leq \left\|\begin{bmatrix}I_n & \mathbf{0} \\ \mathbf{0} & \mathbf{0}\end{bmatrix}(T_c^T\otimes I_n)A_{c,k}(T_c\otimes I_n)\right. \\ &\quad \left.\times\begin{bmatrix}\mathbf{0} & \mathbf{0} \\ \mathbf{0} & I_{n(N-1)}\end{bmatrix}\right\|_{I_N\otimes P}\left\|\begin{bmatrix}\mathbf{0} \\ \Lambda_{p,k}^r\eta_k\end{bmatrix}\right\|_{I_N\otimes P} \\ &\leq \|A_{c,k}\|_{I_N\otimes P}\|\Lambda_{p,k}\|_{I_{N-1}\otimes P}^r\|\eta_k\|_{I_{N-1}\otimes P}.\end{aligned}$$

Consequently, since $\|A_{c,k}\|_{I_N\otimes P} \leq \bar{a}$ and $\|\Lambda_{p,k}\| \leq \theta$, the expression (41) becomes:

$$\|\varepsilon_{k+1}\|_P \leq \sqrt{\lambda}\|\varepsilon_k\|_P + \bar{a}\theta^r\|\eta_k\|_{I_{N-1}\otimes P}. \tag{42}$$

Now, by combining Eqs. (40) and (42), we obtain

$$\begin{bmatrix}\|\varepsilon_{k+1}\|_P \\ \|\eta_{k+1}\|_{I_{N-1}\otimes P}\end{bmatrix} \leq \underbrace{\begin{bmatrix}\sqrt{\lambda} & \bar{a}\theta^r \\ \bar{a} & \bar{a}\theta^r\end{bmatrix}}_{:=\Gamma(r)}\begin{bmatrix}\|\varepsilon_k\|_P \\ \|\eta_k\|_{I_{N-1}\otimes P}\end{bmatrix}. \tag{43}$$

The above is a recursive inequality of the form: $\psi_{k+1} \leq \Gamma(r)\psi_k$, where $\psi_k = (\|\varepsilon_k\|_P, \|\eta_k\|_{I_{N-1}\otimes P}) \geq 0$ (element-wise) and $\Gamma(r) \geq 0$ (element-wise) with $\psi(0) \geq 0$. Note that, since λ and θ are both in $[0, 1)$, r can be chosen large enough such that $\sigma(\Gamma(r)) \subset (-1, 1)$. This follows from the fact that the eigenvalues of $\Gamma(r)$, $s_{1,2}$, are given as

$$s_{1,2}(r) = \frac{1}{2}(\bar{a}\theta^r + \sqrt{\lambda}) \pm \frac{1}{2}\sqrt{(\bar{a}\theta^r - \sqrt{\lambda})^2 + 4\bar{a}^2\theta^r}.$$

Since $\bar{a}$ and θ are positive, simple inspection reveals that both eigenvalues are real numbers. Furthermore

$$\lim_{r\to\infty} s_1(r) = \sqrt{\lambda} \quad \text{and} \quad \lim_{r\to\infty} s_2(r) = 0.$$

Since $s_{1,2}$ are continuous function of r, the above implies that there exists large enough r such that $|s_{1,2}(r)| < 1$. Next, since $\Gamma(r)$ has positive entries, $\psi_k \leq \Gamma(r)\psi_{k-1} \leq \Gamma(r)^2\psi_{k-2} \leq \cdots \leq \Gamma(r)^k\psi_0$. Since $\sigma(\Gamma(r)) \subset (-1, 1)$, and hence $\lim_{k\to\infty}\Gamma(r)^k = 0$, which implies that $\lim_{k\to\infty}\psi_k = 0$. This then implies stability with $\lim_{k\to\infty}\psi_k = 0$ exponentially. ■

Theorem 2 implies that r can be chosen large enough such that $\rho(\Gamma(r)) < 1$ to ensure the exponential stability of the error dynamics, which can be done via a line search on r as shown on an example case in Fig. 4. Hence, we now have a decentralized observer synthesis described as follows.

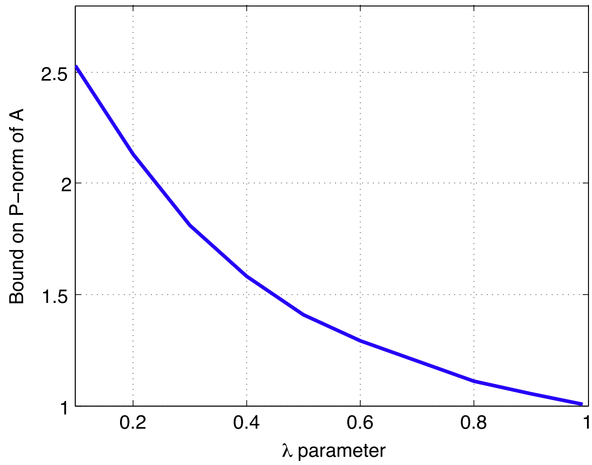

Fig. 3. An example of λ versus $\|A\|_P \leq \bar{a}$ for $N = 8$.

Algorithm 1.

- *Step* 1: Solve for θ and δ using Eqs. (36) and (37).
- *Step* 2: Perform a line search over $\lambda \in [0, 1)$ to determine the smallest integer $r \geq 1$ such that $\rho(\Gamma(r)) < 1$: for each λ, perform a line search on $\bar{a}$ and determine the pair $(\lambda, \bar{a})$ for which inequalities (30) and (34) are jointly feasible for $P = P^T > 0$ and S. Then compute the smallest r such that $\rho(\Gamma(r)) < 1$ ($\Gamma(r)$ is given by (38)).

λ, $\bar{a}$, r, are computed by the algorithm via multiple line searches with the following order: the highest level line search is for λ. Then for each λ there is a line search for $\bar{a}$. Since r is a positive integer, for each pair of $(\lambda, \bar{a})$, the computation of smallest r requires minimal computation. Note that, using (43), λ is the exponential decay rate for the agreement dynamics, that is, $\|\varepsilon_{k+1}\|_P \leq \sqrt{\lambda}\|\varepsilon_k\|_P$ when $\eta_k = \mathbf{0}$, with $\lambda \in [0, 1]$. This implies that reducing λ towards zero increases the exponential decay rate of the agreement dynamics, and hence it would also reduce the value of r (see Eq. (38)) needed for the stability of the overall observer. This can also be observed from the form of the matrix $\Gamma(r)$, where the reduction in λ allows smaller r values for the satisfaction of $\rho(\Gamma(r)) < 1$.

6. Impact of communication topology on consensus

This section discusses how the specific structure of the communication graph can be exploited to find less conservative bounds on the number of consensus iterations, r, needed for the exponential stability of the observer. For illustration, we consider $N = 8$ with $\lambda = 0.9$.

First, it is assumed that a specific connected communication subgraph is contained in all communications graphs. This implies that all other communication graphs are simply obtained by adding connections to this subgraph. The following result states that the algebraic connectivity is then bounded from below by this subgraph, which is used to obtain tighter lower bounds on the Laplacian eigenvalues.

Proposition 1. *Adding a new edge to a connected graph will not decrease its algebraic connectivity.*

Proof. Consider a graph with Laplacian $\mathcal{L}_c$. Suppose we introduce additional links, which add to the Laplacian with $\Delta := \sum_{(i,j)\in E_\delta} (e_i - e_j)(e_i - e_j)^T$ for additional set of edges E_δ, such that $\mathcal{L}_a = \mathcal{L}_c + \Delta$ is the new Laplacian. The following hold: $\mathcal{L}_c$, $\mathcal{L}_a$, and Δ are positive semidefinite matrices and the vector $\mathbf{1}$ is in each's null space. Let λ_a and λ_c be algebraic connectivities, $\mathbf{a}$, of $\mathcal{L}_c$ and $\mathcal{L}_a$ with v_c and v_a are the corresponding eigenvectors. Note that $v_a^T\mathbf{1} = v_c^T\mathbf{1} = 0$ since eigenvectors of symmetric matrices form an orthogonal set of vectors and $\mathbf{1}$ is an eigenvector for both Laplacians. Consider a similarity transformation P as follows: $P = [P_r \mid \mathbf{1}/\sqrt{n}]$ where P_r is a one-to-one matrix such that $P_r^T\mathbf{1} = \mathbf{0}$ and $P_r^T P_r = I$. Then $P^{-1} = P^T$. Since $\mathbf{1}$ is in the null space of the Laplacians, e.g., $\mathcal{L}_c\mathbf{1} = \mathbf{0}$ and $\mathbf{1}^T\mathcal{L}_c = \mathbf{0}^T$, $\tilde{\mathcal{L}}_c = P^T\mathcal{L}_c P$ has the following form

$$\tilde{\mathcal{L}}_c = \begin{bmatrix} \tilde{\mathcal{L}}_{c,p} & P_r^T\mathcal{L}_c\mathbf{1}/\sqrt{n} \\ \mathbf{1}^T\mathcal{L}_c P_r/\sqrt{n} & \mathbf{1}^T\mathcal{L}_c\mathbf{1}/n \end{bmatrix} = \begin{bmatrix} \tilde{\mathcal{L}}_{c,p} & \mathbf{0} \\ \mathbf{0} & 0 \end{bmatrix}$$

where $\tilde{\mathcal{L}}_{c,p} = P_r^T\mathcal{L}_c P_r$. By using this similarity transformation, we can define $\tilde{\mathcal{L}}_a$, $\tilde{\mathcal{L}}_{a,p}$, and $\tilde{\Delta}$, $\tilde{\Delta}_p$, i.e., $\tilde{\mathcal{L}}_a = P^T\mathcal{L}_a P$ and $\tilde{\Delta} = P^T\Delta P$. Both matrices will have the same block-diagonal structure as $\tilde{\mathcal{L}}_c$ with $\tilde{\mathcal{L}}_{c,p}$ replaced by $\tilde{\mathcal{L}}_{a,p} = P_r^T\mathcal{L}_a P_r$ and $\tilde{\Delta}_p = P_r^T\Delta P_r$. Note that $\tilde{\mathcal{L}}_{a,p} \geq \lambda_a I$, $\tilde{\mathcal{L}}_{c,p} \geq \lambda_c I$, and $\tilde{\Delta}_p \geq 0$. Observe that, since $\mathbf{1}^T v_a = 0$, $P^T v_a = (\tilde{v}_a, 0)$ for some $\tilde{v}_a$ and $\tilde{\mathcal{L}}_a = \tilde{\mathcal{L}}_c + \tilde{\Delta}$. Combining these observations

$$\begin{aligned}\lambda_a &= v_a^T PP^T\mathcal{L}_a PP^T v_a \geq v_a^T PP^T\mathcal{L}_c PP^T v_a \\ &= \tilde{v}_a^T\tilde{\mathcal{L}}_{c,p}\tilde{v}_a \geq \lambda_c,\end{aligned}$$

which implies $\lambda_a \geq \lambda_c$, which concludes the proof. ■

Table 1
Algebraic connectivity and consensus bounds, as predicted by Algorithm 1, for various communication graphs.

Topology type	$\mathbf{a}(\mathbf{G})$	θ $(N = 8)$	r $(N = 8)$
Path	$2(1 - \cos(\pi/N))$	0.96	76
Cycle	$2(1 - \cos(2\pi/N))$	0.91	33
Star	1	0.86	21
Complete	N	0.27	3
Cube (m-dim)	2	0.75	11

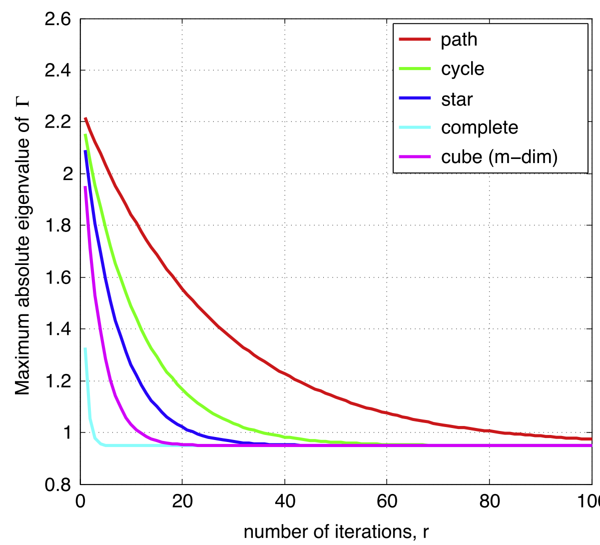

Fig. 4. Maximum absolute eigenvalue of the $\Gamma(r; L, \delta)$ matrix for the example of 8 agents and various topologies.

Table 1 presents the number of consensus iterations needed in this example, when such a common subgraph (with path, cycle, star, complete, and cube topologies) is shared among all graphs. The tighter lower bound due to the algebraic connectivity is used with a bound $\bar{a}$ on $\|A\|_P$, which is computed as described in Algorithm 1 (see Fig. 3). Fig. 4 shows $\rho(\Gamma(r))$ as a function of r for different topologies, which is then used to construct this table.

As Table 1 and Fig. 4 imply, for a given λ and hence $\bar{a}$, the values of θ and r can vary significantly as a function of the communication topology. If there is additional information on all possible communication topologies, we can obtain a smaller value for θ, which in return implies a smaller value of r. The value of θ decreases as the gap between the values of $\underline{b}$ and $\bar{b}$ gets smaller, as determined by Eq. (36), which in return implies smaller values of r. Next we present several examples where this observation is exploited when a specific communication graph persists over time.

Example 1. The cube topology of dimension m, Q_m, has a fixed lower bound on the algebraic connectivity, $\mathbf{a}(Q_m)$, but also a much smaller upper bound on the maximum eigenvalue of its Laplacian matrix, than predicted by Eq. (49) in the Appendix. In fact, all the eigenvalues of Q_m are known (Chung, 1994; Mohar, 1997) as, $\lambda(\mathcal{L}(Q_m)) = 2k$ with multiplicity $\binom{m}{k}$ for $k = 0 \dots m$. This implies, for instance, that a cube Q_3 has $\mathbf{a}(Q_3) = 2$ and $\max(\sigma(\mathcal{L}(Q_3))) = 6$, rather than 0.15 and 14, respectively, as predicted by Eqs. (48) and (49). Consequently, the new bounds on the eigenvalues of the cube Laplacian provide $\theta = 0.5$ and hence $r = 5$ instead of $r = 11$, which is shown in Fig. 5. Also note that the bounds for the cube communication topology are independent of the number of agents N, and hence stay the same as the number of agents increases. This means that the number of iterations required would remain the same as the number of agents increase as long as λ and $\bar{a}$ do not change.

Example 2. The star topology with N number of vertices, G_{Star_N}, has eigenvalues of its Laplacian at 0, 1 (with multiplicity $N-2$) and N (Chung, 1994). Hence $\mathbf{a}(G_{\mathrm{Star}_N}) = 1$ and $\max(\sigma(\mathcal{L}(G_{\mathrm{Star}_N}))) = N$, leading to tighter bounds than predicted by Eqs. (48) and (49) in the Appendix. For $N = 8$, the value of $\theta = 0.78$ and the number of consensus iterations is $r = 12$. This is also shown in Fig. 5.

Example 3. For a fully connected topology with N vertices, all the non-zero eigenvalues of the corresponding Laplacian are equal to N, which implies that $\underline{b} = \bar{b}$, with $\theta = 0$ and $\delta = 1/N$. This is intuitive, because all agents communicate with each other and the consensus is immediately achieved as the simple average of all the communicated information. Therefore choosing $r = 1$ is sufficient for observer stability.

In summary, decreasing the gap between the algebraic connectivity and maximum eigenvalue of a graph's Laplacian matrix is important as it allows to reduce θ term. Therefore, if we design communication topologies containing a graph with a large algebraic connectivity (such as cube or star topology), the eigenvalues can be controlled as adding new edges will not decrease the algebraic connectivity. Furthermore, in practice, it is observed that only a few consensus iterations are actually needed (see Section 7), which is far less than what the theoretical bounds above predict.

7. Numerical example

This section presents an example of spacecraft in Low Earth Orbit (LEO) to demonstrate the performance of the decentralized observer with the consensus filter. We assume a group of N spacecraft with time-varying sensing topology defined by the graphs $\mathbf{G}_{s,k}$, $k = 0, 1, \dots$, and communication topology $\mathbf{G}_{c,k}$, $k = 0, 1, \dots$. According to $\mathbf{G}_{c,k}$ each vehicle i, where $i = 1 \dots N$, has a set of neighbors $S_{i,k}$. The state vector to be estimated consists of the relative positions and velocities of all vehicles with respect to the central vehicle (i.e., vehicle 1). Therefore, the state vector size is $n = 6(N-1)$. The relative translational state of the formation is defined as the vector of positions and velocities of each spacecraft relative to the reference spacecraft in the formation, which is designated with the index 1 without loss of generality (Açıkmeşe, Scharf, Carson, & Hadaegh, 2008; Sukhatme, 2009). Specifically,

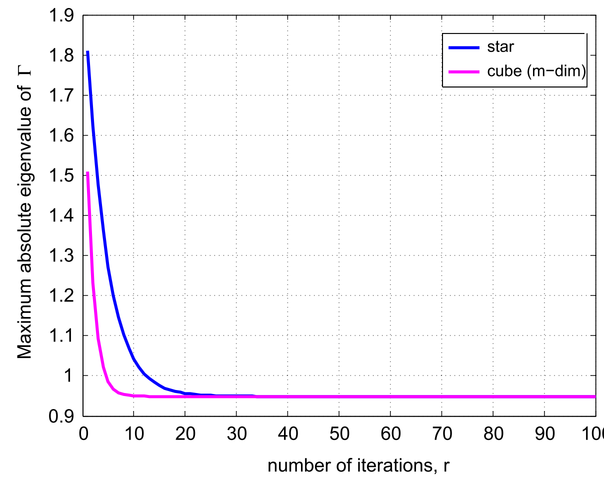

Fig. 5. Maximum absolute eigenvalue of the $\Gamma(r; L, \delta)$ matrix for the example of 8 agents, with special case communication topologies, star and cube, as stated in Examples 1 and 2.

$$x = \left[p_{12,1} \ \dots \ p_{1N,1} \,\middle|\, p_{12,2} \ \dots \ p_{1N,2} \,\middle|\, \dots \middle|\, v_{12,3} \ \dots \ v_{1N,3} \right]^T \tag{44}$$

where N is the number of spacecraft in the formation, and

$$p_{ij} = \begin{bmatrix} p_{ij,1} \\ p_{ij,2} \\ p_{ij,3} \end{bmatrix}, \qquad v_{ij} = \begin{bmatrix} v_{ij,1} \\ v_{ij,2} \\ v_{ij,3} \end{bmatrix},$$
$$i \neq j, \ i = 1, \dots, N-1, \ j = 2, \dots, N, \tag{45}$$

where $p_{ij,k}$ ($v_{ij,k}$), $k = 1, 2, 3$, is the kth coordinate of the position (velocity) of the jth relative to the ith spacecraft.

The discrete time dynamics for the relative formation state is given by Eq. (1) where A matrix is defined as

$$A = e^{A_0 \Delta t} \otimes I_{N-1} \tag{46}$$

A_0 represents the linearized orbital dynamics (Açıkmeşe et al., 2008)

$$A_0 = \begin{bmatrix} 0_3 & I_3 \\ \omega^2 D_0 & \omega S_0 \end{bmatrix}, \qquad D_0 = \begin{bmatrix} 3 & 0 & 0 \\ 0 & 0 & 0 \\ 0 & 0 & -1 \end{bmatrix},$$

$$S_0 = \begin{bmatrix} 0 & 2 & 0 \\ -2 & 0 & 0 \\ 0 & 0 & 0 \end{bmatrix},$$

$\omega = \sqrt{\mu/R^3}$, R is the radius of the orbit and μ is the gravitational parameter of the primary body, I_m and 0_m are the $m \times m$ identity and zero matrices. Finally, the measurement model is given by Eq. (2). The measured output is a linear, time-varying function of the state. C_k is a time-varying matrix corresponding to time-varying sensor graphs topology $\mathbf{G}_{s,k}$, which is a pseudo-connected undirected graph. Measurements can be obtained by a variety of formation sensors and can be of different type. Without loss of generality, we assume that the measurements from each sensor give a relative position vector between a pair of agents, and that the measurement is available to both agents.

7.1. Algorithm performance under parameter variations

The simulation results show the effect of the observer convergence rate parameter, λ, and number of consensus iterations, r on convergence and consensus of the local observers. We show that

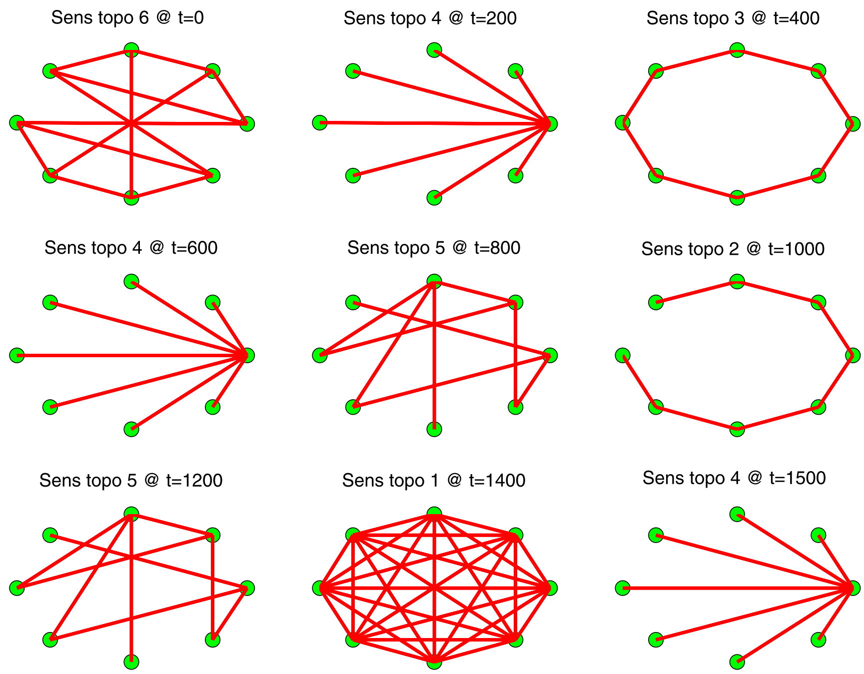

Fig. 6. Sensing topology.

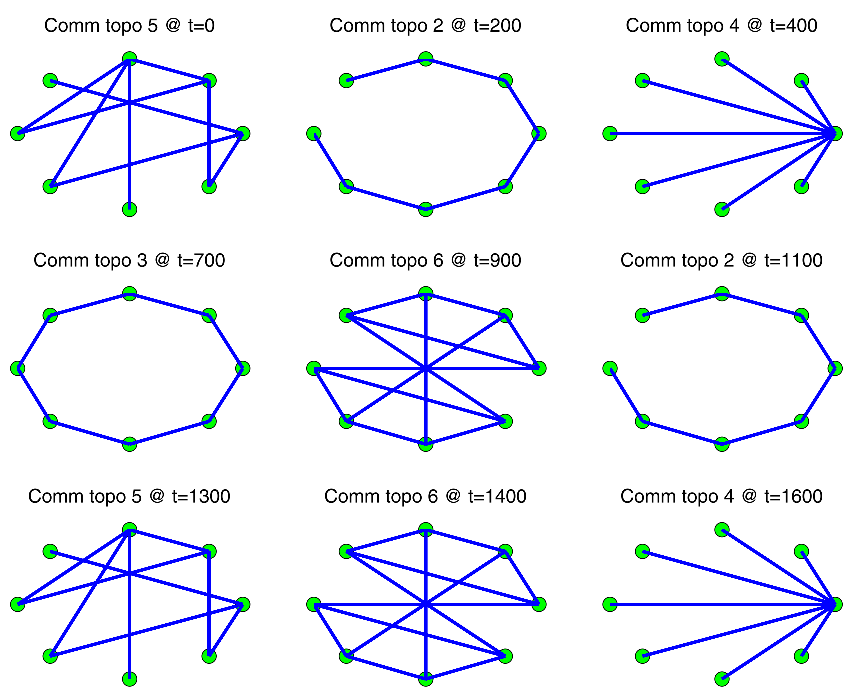

Fig. 7. Communication topology.

the parameter λ can control convergence rates and that the parameter r plays an important role in achieving stability of the observer and faster agreement among the agents' estimates. We also show that only a relatively low number of iterations is required to reach a consensus, which implies lower communication bandwidth. This can be useful for algorithm's applicability to real systems. Additional simulation results can be found in Mandić, Açıkmeşe, and Speyer (2010).

Applying the approach described in the Algorithm 1, we compute the θ, δ and $\bar{a}$ parameters, as well as the bound on consensus iterations. In these simulations, $h_{i,k} = 2$, $\forall i, k$, i.e., if there exist a relative measurement between two spacecraft, both spacecraft have access to it. Simulations show that the algorithm works well even with only $r = 3$ though the theory predicts higher number of iterations for certain topologies.

The results are shown for the $\Delta t = 1$ s with 8 spacecraft. The sensing and communication topologies change according to Figs. 6 and 7. Both topologies may or may not change at the same time. The time of topology change is indicated in the error-plots with the blue circle and red dot, for communication and sensing topology changes respectively. Also note that the communication topologies in Fig. 7 represent, graphically, the communication graphs directly.

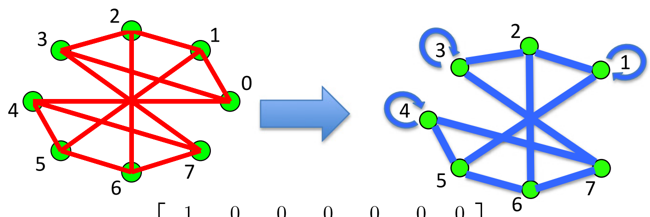

$$E = \begin{bmatrix} 1 & 0 & 0 & 0 & 0 & 0 & 0 \\ 0 & 0 & 1 & 0 & 0 & 0 & 0 \\ 0 & 0 & 0 & 1 & 0 & 0 & 0 \\ -1 & 1 & 0 & 0 & 0 & 0 & 0 \\ -1 & 0 & 0 & 0 & 1 & 0 & 0 \\ 0 & -1 & 1 & 0 & 0 & 0 & 0 \\ 0 & -1 & 0 & 0 & 0 & 1 & 0 \\ 0 & 0 & -1 & 0 & 0 & 0 & 1 \\ 0 & 0 & 0 & -1 & 1 & 0 & 0 \\ 0 & 0 & 0 & -1 & 0 & 0 & 1 \\ 0 & 0 & 0 & 0 & -1 & 1 & 0 \\ 0 & 0 & 0 & 0 & 0 & -1 & 1 \end{bmatrix}$$

Fig. 8. Sensing graph example. E is vertex-adjacency matrix for the sensing graph with self-loops.

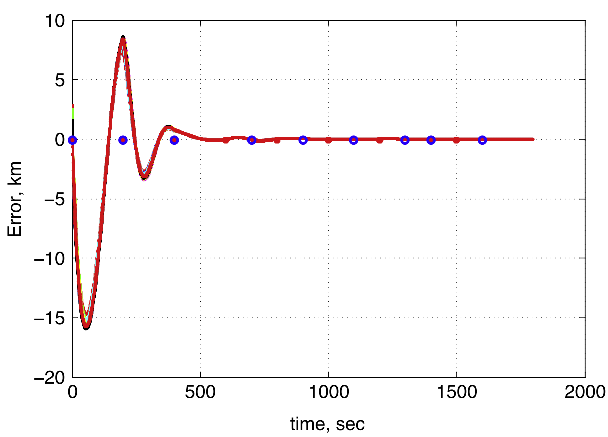

Fig. 9. $\lambda = 0.90, r = 11$.

On the other hand the sensing topologies do not have the same interpretation: a connection between each spacecraft represents a relative measurement. The conversion of a sensing topology to a sensing graph and the corresponding vertex-adjacency matrix is given in Fig. 8.

Figs. 9 and 10 show the performance of the algorithm for $\lambda = 0.90$ and $\lambda = 0.80$ respectively, with number of iterations set to $r = 11$. It is worth noting the improvement in convergence when $\lambda = 0.80$ by observing the transient times in both cases. For the case with $\lambda = 0.80$ the first crossing of the x-axis occurs at around 80 s, while in the case $\lambda = 0.90$ it takes about 140 s. On the other hand, to decrease the communication bandwidth needed and speed up the execution, we set $r = 3$. Fig. 11 shows that the consensus is reached and algorithm converges. Each spacecraft exchanges enough information with other spacecraft to maintain a stable observer. During the transient the consensus is not achieved as fast as in previous cases, which is expected with decreased number of iterations. But decreasing the number of iterations further can be harmful, and in the case when $r = 1$ and $\lambda = 0.90$ the observer becomes unstable, as shown in Fig. 12.

8. Conclusions

The decentralized observer with consensus filter proposed here provides a computationally efficient estimation technique for handling time-varying sensing and communication topologies for distributed systems. The method is computationally efficient and it does not require onboard gain computation. The observer gains are computed offline by solving an LMI feasibility problem. The implementation of the algorithm requires minimal communication load, which makes the algorithm suitable for realtime systems with low communication bandwidth. Simulation results for a set of eight spacecraft are presented to support the convergence results of the algorithm.

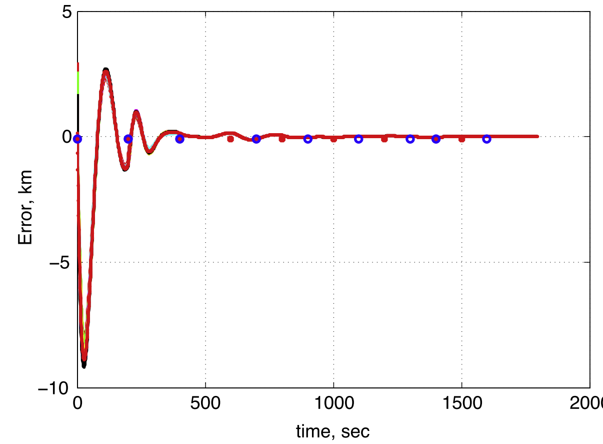

Fig. 10. $\lambda = 0.80, r = 11$.

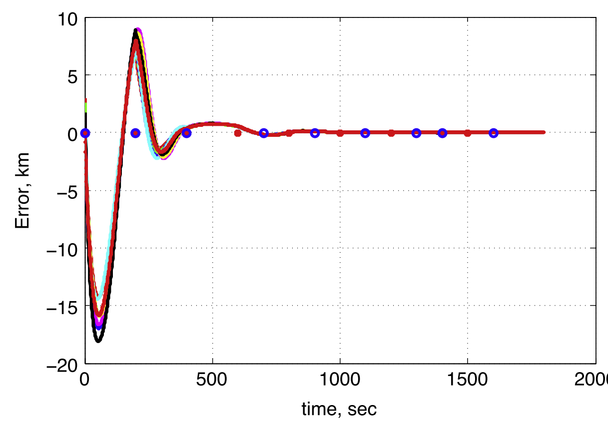

Fig. 11. $\lambda = 0.90, r = 3$.

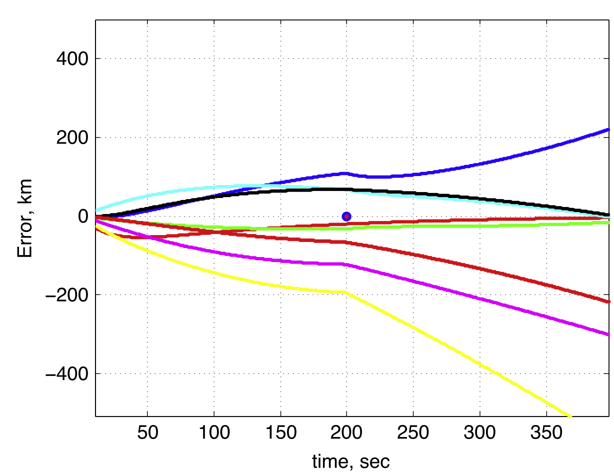

Fig. 12. $\lambda = 0.90, r = 1$.

Future work may include: (i) considering process and measurement noise in the decentralized observer design; (ii) obtaining tighter bounds on the number of consensus iterations by exploiting the structure of the specific communication graphs at hand; (iii) a comparative study of communication complexity for consensus based decentralized observers with a simple communication routing scheme, as studied in this paper, and observers requiring the routing of all the measurements with a more complex routing scheme.

Acknowledgments

We are thankful to David S. Bayard of JPL for his valuable comments and suggestions. We are also grateful for the anonymous reviewers' detailed and constructive comments and suggestions, which improved the clarity and the quality of the paper. This research was performed partially at the Jet Propulsion Laboratory, California Institute of Technology, under a contract with the National Aeronautics and Space Administration. ©2014 California Institute of Technology.

Appendix. Graph theoretic concepts and Laplacian of graphs with self-loops

In this section we will introduce some known facts about graph theory with a new result on graphs with self-loops. For graphs with self-loops, we will introduce the concept of pseudo connectedness, which is useful in our developments.

Let $\mathbf{G} = (\mathbf{V}, \mathbf{E})$ represents a finite graph with a set of vertices $\mathbf{V}$ and edges $\mathbf{E}$ with $(i, j) \in \mathbf{E}$ denoting an edge between the vertices i and j. $\mathcal{L}(\mathbf{G})$ is the Laplacian matrix for the graph $\mathbf{G}$; $\mathbf{a}(\mathbf{G})$ is the algebraic connectivity of the graph G, which is the second smallest eigenvalue of $\mathcal{L}(\mathbf{G})$. E is the vertex–edge adjacency matrix, which is described later on in Section 1.1, $\mathcal{A}$ is the adjacency matrix, and $\mathcal{D}$ is the diagonal matrix of node in-degrees for $\mathbf{G}$, then the following gives a relationship to compute the Laplacian matrix

$$\mathcal{L}(\mathbf{G}) = E^T E = \mathcal{D} - \mathcal{A}. \tag{47}$$

The following relationships are well known in the literature (Fiedler, 1973; Horn & Johnson, 1999) for a connected undirected graph $\mathbf{G}$ with N vertices and without any *self-loops or multiple edges*

$$\mathbf{a}(\mathbf{G}) \geq 2(1 - \cos(\pi/N)) \tag{48}$$

$$2\mathbf{d}(\mathbf{G}) \geq \max(\sigma(\mathcal{L}(\mathbf{G}))), \tag{49}$$

where $\mathbf{d}(\mathbf{G})$ is the maximum in-degree of $\mathbf{G}$. Indeed the inequality (49) is valid for any undirected graph without self-loops or multiple edges whether they are connected or not. Also, due to the connectedness of the graph, the minimum eigenvalue of the Laplacian matrix is 0 with algebraic multiplicity of 1 and the eigenvector of $\mathbf{1}$. Next we characterize the location of the Laplacian eigenvalues for a connected undirected graph $\mathbf{G}$ with self-loops. Having a self-loop does not change whether a graph is connected or not, that is, a graph with self-loops is connected if and only if the same graph with the self-loops removed is connected. Furthermore, we define the Laplacian of an undirected graph with at least one self-loop as

$$\mathcal{L}(\mathbf{G}) = \mathcal{L}(\mathbf{G}^o) + \sum_{(i,i)\in\mathbf{E}} \mathbf{e}_i \mathbf{e}_i^T \tag{50}$$

where $\mathbf{G}^o$ is the largest subgraph of $\mathbf{G}$ with the self-loops removed, and

$$\mathcal{L}(\mathbf{G}^o) = \sum_{(i,j)\in\mathbf{E},\, i\neq j} (\mathbf{e}_i - \mathbf{e}_j)(\mathbf{e}_i - \mathbf{e}_j)^T. \tag{51}$$

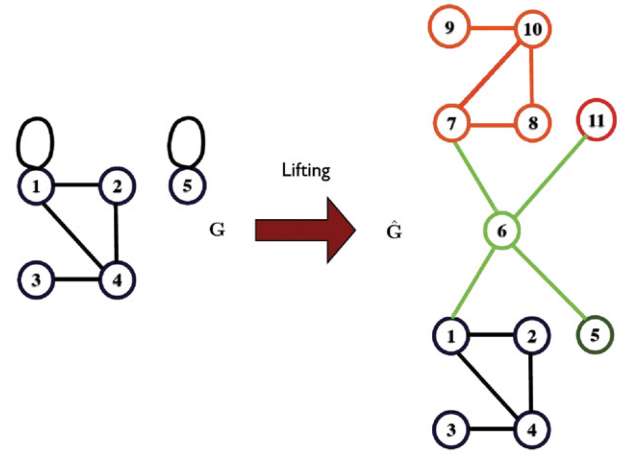

Fig. 13. Lifted graph of a pseudo-connected graph with self-loops.

The following definition introduces the concept of the pseudo-connected graphs, which is our fourth contribution.

Definition 1. An undirected graph $\mathbf{G}(\mathbf{V}, \mathbf{E})$ without multiple edges is *pseudo-connected* if every vertex is connected to itself and/or to another vertex and if every connected subgraph of $\mathbf{G}$ has at least one vertex with a self-loop.

Next we develop useful results on the eigenvalues of undirected graphs with self-loops, which are instrumental in the stability analysis of the decentralized observer. We refer to Mesbahi and Egerstedt (2010) for a graph theoretic view of multi-agent networks.

Lemma 3. *The Laplacian of a pseudo-connected graph is positive definite.*

Proof. A pseudo-connected graph can be partitioned into subgraphs that are connected with at least one self-loop in each subgraph. Note that some of these subgraphs can have a single vertex that has a self-loop. Clearly each subgraph with a single vertex and a self-loop has Laplacian 1. If we can also show that the connected subgraphs that have multiple vertices with at least one self-loop have positive definite Laplacians, then the Laplacian of the overall graph will also be positive definite. This will conclude the proof. To do that we prove that a connected graph $\mathbf{G}$ with at least one self-loop has a positive definite Laplacian. Let $\mathbf{G}^o$ be the connected graph formed by removing the self-loops from $\mathbf{G}$. Any vector $v \neq \mathbf{0}$, which can be expressed as $v = w + \zeta\mathbf{1}$ where $w^T\mathbf{1} = 0$, and either or both $w \neq \mathbf{0}$ and $\zeta \neq 0$. Then, by using (51) $\mathcal{L}(\mathbf{G}) = \mathcal{L}(\mathbf{G}^o) + Q_o$ where $Q_o := \sum_{i=1}^{q} e_i e_i^T$ and q is the number of self-loops and having $\mathbf{1}^T Q_o \mathbf{1} = q$,

$$v^T \mathcal{L}(\mathbf{G}) v = w^T \mathcal{L}(\mathbf{G}^o) w + w^T Q_o w + 2\zeta w^T Q_o \mathbf{1} + q\xi^2 \geq 0.$$

If $w \neq \mathbf{0}$, $w^T \mathcal{L}(\mathbf{G}^o) w > 0$ (due to connectedness of $\mathbf{G}^o$), we have $v^T \mathcal{L}(\mathbf{G}) v > 0$. Next, if $w = 0$ and $\zeta \neq 0$, then $v^T \mathcal{L}(\mathbf{G}) v = q\zeta^2 > 0$. Consequently $\mathcal{L}(\mathbf{G}) = \mathcal{L}(\mathbf{G})^T > 0$, where q is the number of self-loops. ■

Next we introduce the concept of *lifted graph* to characterize the eigenvalues of the Laplacian of a graph with self-loops.

Definition 2. Given an undirected graph $\mathbf{G}(\mathbf{E}, \mathbf{V})$ with N vertices and with at least one self-loop, its lifted graph $\hat{\mathbf{G}}(\hat{\mathbf{E}}, \hat{\mathbf{V}})$ is a graph with $2N + 1$ vertices and with no self-loops such that (Fig. 13): For every vertex i in $\mathbf{G}$ there are vertices i and $i + N + 1$ in $\hat{\mathbf{G}}$,

$i = 1, \ldots, N$, and also a *middle vertex* $N + 1$ with the following edges

$$(i, j) \in \mathbf{E} \Rightarrow (i, j) \in \hat{\mathbf{E}} \quad \text{and} \quad (i + N + 1, j + N + 1) \in \hat{\mathbf{E}}$$
$$(i, i) \in \mathbf{E} \Rightarrow (i, N + 1) \in \hat{\mathbf{E}} \quad \text{and} \quad (N + 1, i + N + 1) \in \hat{\mathbf{E}}.$$

The following theorem is the main result of this section on the eigenvalues of the Laplacians of pseudo-connected graphs, which is our fifth key contribution.

Theorem 3. *For a finite undirected graph,* $\mathbf{G}$, *with self-loops but without multiple-edges:*

$$\sigma\left(\mathcal{L}(\mathbf{G})\right) \subseteq \sigma\left(\mathcal{L}(\hat{\mathbf{G}})\right) \cap [0, 2\mathbf{d}(\mathbf{G}^o) + 1], \tag{52}$$

where $\mathbf{G}^o(\mathbf{V}, \mathbf{E}^o)$ *is a subgraph of* $\mathbf{G}(\mathbf{V}, \mathbf{E})$ *where* $\mathbf{E}^o \subset \mathbf{E}$ *and* $\mathbf{E}^o$ *contains all the edges of* $\mathbf{E}$ *that are not self-loops. Particularly, if* $\mathbf{G}$ *is a pseudo-connected graph, then*

$$\sigma\left(\mathcal{L}(\mathbf{G})\right) \subseteq \sigma_+\left(\mathcal{L}(\hat{\mathbf{G}})\right) \cap [0, 2\mathbf{d}(\mathbf{G}^o) + 1]. \tag{53}$$

Proof. Consider the vertex–edge adjacency matrix E^o for $\mathbf{G}^o$. We have the following relationship for the vertex adjacency matrices of $\mathbf{G}$ and $\hat{\mathbf{G}}$, E and $\hat{E}$, in terms of E^o

$$\hat{E} = \begin{bmatrix} E^o & 0 & 0 \\ S & \mathbf{1} & 0 \\ 0 & \mathbf{1} & S \\ 0 & 0 & E^o \end{bmatrix}, \qquad E = \begin{bmatrix} E^o \\ S \end{bmatrix}$$

where the matrix S has entries of $+1$ or 0. This implies that

$$\mathcal{L}(\hat{G}) = \begin{bmatrix} E^{oT}E^o + S^TS & S^T\mathbf{1} & 0 \\ \mathbf{1}^TS & 2N & \mathbf{1}^TS \\ 0 & S^T\mathbf{1} & E^{oT}E^o + S^TS \end{bmatrix}$$

and $\mathcal{L}(\mathbf{G}) = E^{oT}E^o + S^TS$. Now suppose that $\psi \in \sigma\left(\mathcal{L}(\mathbf{G})\right)$ with the corresponding eigenvector v. Then

$$\mathcal{L}(\hat{\mathbf{G}}) \begin{bmatrix} v \\ 0 \\ -v \end{bmatrix} = \begin{bmatrix} \mathcal{L}(\mathbf{G})v \\ 0 \\ -\mathcal{L}(\mathbf{G})v \end{bmatrix} = \psi \begin{bmatrix} v \\ 0 \\ -v \end{bmatrix}.$$

Consequently $\psi \in \sigma\left(\mathcal{L}(\hat{\mathbf{G}})\right)$ too. Next note that $0 \le S^TS \le I$, which implies that $\mathcal{L}(\mathbf{G}) \le \mathcal{L}(\mathbf{G}^o) + I$. This implies that

$$\max(\sigma\left(\mathcal{L}(\mathbf{G})\right)) \le \max(\sigma(\mathcal{L}(\mathbf{G}^o))) + 1 \le 2\mathbf{d}(\mathbf{G}^o) + 1 \tag{54}$$

which follows from (49). This proves the relationship given by (52). Now by using Lemma 3, the relationship given by (53) directly follows from (52). ■

References

Açıkmeşe, B., & Corless, M. (2008). Stability analysis with quadratic lyapunov functions: a necessary and sufficient multiplier condition. *Systems & Control Letters*, *57*, 78–94.

Açıkmeşe, B., & Corless, M. (2011). Observers for systems with nonlinearities satisfying incremental quadratic constraints. *Automatica*, *47*(7), 1339–1349.

Açıkmeşe, B., Scharf, D. P., Carson, J. M., & Hadaegh, F. Y. (2008). Distributed estimation for spacecraft formations over time-varying sensing topologies. In *Proceedings of the 17th IFAC world congress* (pp. 2123–2130).

Anderson, D. B. D. O., & Moore, J. B. (1979). *Optimal filtering*. Englewood Cliffs, NJ: Prentice-Hall.

Arambel, P. O., Rago, C., & Mehra, R. K. (2001). Covariance intersection algorithm for distributed spacecraft state estimation. In *Proc. American control conf.*: *Vol. 6* (pp. 4398–4403).

Boyd, S., El Ghaoui, L., Feron, E., & Balakrishnan, V. (1994). *Linear matrix inequalities in system and control theory*. SIAM.

Chen, L., Arambel, P. O., & Mehra, R. K. (2002). Estimation under unknown correlation: covariance intersection revisited. *IEEE Transactions on Automatic Control*, *47*(11), 1879–1882.

Chung, R. K. (1994). *CBMS*, *Spectral graph theory*. American Mathematical Society.

Das, A. K., & Mesbahi, M. (2006). Distributed linear parameter estimation in sensor networks based on Laplacian dynamics consensus algorithm. In *3rd Annual IEEE communications society on sensor and adhoc communications and networks* (pp. 440–449).

Deo, N. (1974). *Graph theory with applications to engineering and computer science*. Prentice-Hall.

Fiedler, M. (1973). Algebraic connectivity of graphs. *Czechoslovak Mathematical Journal*, *23*(2), 298–305.

Hatano, Y., & Mesbahi, M. (2005). Agreement over random networks. *IEEE Transactions on Automatic Control*, *50*(11), 1867–1872.

Horn, R. A., & Johnson, C. R. (Eds.) (1999). *Matrix analysis*. New York: Cambridge University Press.

Jadbabaie, A., Lin, G. J., & Morse, A. S. (2003). Coordination of groups of mobile autonomous agents using nearest neighbor rules. *IEEE Transactions on Automatic Control*, *48*(6), 988–1001.

Jazwinski, A. H. (1970). *Stochastic processes and filtering theory, Vol. 63*. Academic Press.

Kamgarpour, M., & Tomlin, C. (2008). Convergence properties of a decentralized Kalman filter. In *IEEE Conference on decision and control* (pp. 3205–3210).

Khan, U. A., & Jadbabaie, A. (2011). On the stability and optimality of distributed Kalman filters with finite-time data fusion? In *American control conference* (pp. 3405–3410).

Mandić, M., Açıkmeşe, B., & Speyer, J. L. (2010). Application of a decentralized observer with a consensus filter to distributed spacecraft systems. In *GN&C AIAA conference*.

Mesbahi, M., & Egerstedt, M. (2010). *Graph theoretic methods in multiagent networks*. Princeton University Press.

Mohar, B. (1997). Some applications of laplace eigenvalues of graphs. *NATO ASI*, *497*(Ser. C), 225–275.

Mutambara, A. G. O. (1998). *Decentralized estimation and control for multisensor systems*. CRC Press LLC.

Olfati-Saber, R. (2005). Distributed Kalman filtering with embedded consensus filters. In *Proc. of the 44th IEEE conference on decision and control*.

Olfati-Saber, R. (2007). Distributed Kalman filtering for sensor networks. In *Proc. of the 46th IEEE conference on decision and control*.

Olfati-Saber, R., Fax, J. A., & Murray, R. M. (2007). Consensus and cooperation in networked multi-agent systems. *Proceedings of the IEEE*, *95*(1), 215–233.

Olfati-Saber, R., & Murray, R. M. (2004). Consensus problems in networks of agents with switching topology and time-delays. *IEEE Transactions on Automatic Control*, *49*(9), 1520–1533.

Ren, W., & Beard, R. W. (2005). Consensus seeking in multi-agent systems under dynamically changing interaction topologies. *IEEE Transactions on Automatic Control*, *50*(5), 655–661.

Shi, L., Johansson, K. H., & Murray, R. M. (2008). Estimation over wireless sensor networks: trades between communication, computation and estimation qualities. In *Proceedings of the 17th IFAC world congress, Seoul, Korea* (pp. 605–611).

Siljak, D. (1978). *Large-scale dynamics systems: stability and structure*. New York: North-Holland.

Smith, R. S., & Hadaegh, F. Y. (2007). Closed-loop dynamics of cooperative vehicle formations with parallel estimators and communication. *IEEE Transactions on Automatic Control*, *52*(8), 1404–1414.

Speyer, J. L. (1979). Communication and transmission requirements for a decentralized linear quadratic-Gaussian control problem. *IEEE Transactions on Automatic Control*, *24*(2), 266–269.

Subbotin, M. V., & Smith, R. S. (2009). Design of distributed decentralized estimators for formations with fixed and stochastic topologies. *Automatica*, *45*(11), 2491–2501.

Sukhatme, G. S. (Ed.) (2009). *The path to autonomous robots*. New York: Springer.

Willsky, A. S., Bello, M. G., Castanon, D. A., Levy, B. C., & Verghese, G. C. (1982). Combining and updating of local estimates and regional maps along sets of one-dimensional tracks. *IEEE Transactions on Automatic Control*, *27*(4), 799–813.

Xiao, L., Boyd, S., & Kim, S.-J. (2007). Distributed average consensus with least-mean-square deviation. *Journal of Parallel and Distributed Computing*, *67*(1), 33–46.

Behçet Açıkmeşe received his Ph.D. in Aerospace Engineering from Purdue University. He was a Visiting Assistant Professor of Aerospace Engineering at Purdue University before joining NASA Jet Propulsion Laboratory (JPL) in 2003. At JPL, he developed the autonomous sky-crane flyaway control algorithms used to successfully land the Curiosity rover on Mars in August 2012. He also developed reaction control system flight control algorithms for NASA SMAP mission scheduled to be launched to orbit in 2014. He joined the faculty of the Department of Aerospace Engineering and Engineering Mechanics at the University of Texas at Austin in 2012, where he is conducting research in robust and nonlinear control, distributed systems, real-time convex optimization and linear matrix inequalities (LMIs) applied to control systems. He is an Associate Fellow of AIAA.

Milan Mandić is an Analyst in Guidance and Control Analysis Group at NASA JPL. He finished his Ph.D. at UCLA in Mechanical engineering and his M.Sc. and B.Sc. at MIT. His interests are in areas of distributed estimation for formation flying spacecraft, and in high precision pointing for space and balloon-borne observatories. Currently, he is the PI of STABLE project, a technology demonstration of sub-arcsecond precision pointing instrument onboard the high altitude balloon and is the lead for the Pointing Control Subsystem.

Jason L. Speyer received the B.S. in Aeronautics and Astronautics from MIT, and the Ph.D. in applied mathematics from Harvard University. He is the Ronald and Valerie Sugar Distinguished Professor in Engineering within the Mechanical and Aerospace Engineering Department and the Electrical Engineering Department, UCLA. He coauthored, with W. H. Chung, Stochastic Processes, Estimation, and Control (SIAM, 2008), and coauthored, with D. H. Jacobson, Primer on Optimal Control Theory (SIAM, 2010). He is a life fellow of the IEEE and a fellow of the AIAA and was awarded the AIAA Mechanics and Control of Flight Award, AIAA Dryden Lectureship in Research, Air Force Exceptional Civilian Decoration (1991 and 2001), IEEE Third Millennium Medal, the AIAA Aerospace Guidance, Navigation, and Control Award, and membership in the National Academy of Engineering.